New friction factor correlation for phase-change flow in plate heat exchangers

Yagnavalkya Mukkamala[a*], Jaco Dirker[b]

[a]School of Mechanical Engineering, Vellore Institute of Technology, Vellore, India

[b]Department of Mechanical and Aeronautical Engineering, University of Pretoria, South Africa

ABSTRACT

This article reports a new two-phase friction factor correlation for condensing and evaporating flows in plate heat exchangers. Over a thousand condensation pressure drop data compiled from seventeen articles were reduced to a two-phase friction factor correlation and successfully evaluated with data not used for correlation development. Similarly, over two thousand evaporation pressure drop data were collected from twenty-four articles and were empirically modeled to yield a two-phase friction factor, which was also successfully validated with independent data. The condensation friction factor correlation fit 72% of the data within ±50% and modeled 92% of the evaluation data within ±50%. Similarly, the evaporation friction factor correlation fit 64.9% of the data within ±50% and 89.8% of the evaluation data within ±50%. Pressure drop in condensers was predominantly due to convective condensation and buoyancy forces. Inertial forces and convective boiling were mainly responsible for the pressure drop in evaporators. As the Weber number was much less than one, drop condensation and nucleate boiling were insignificant. Meta-analysis strongly recommended deploying plate heat exchangers as condensers for lowering the pressure drop and was inconclusive for evaporators.

∗Corresponding Author. Address: School of Mechanical Engineering, Vellore Institute of Technology, Vellore 632014, India; Phone: 91-9345310732; 91-0416-2202203; e-mail: yagnasmukkamala@vit.ac.in; Fax: 91-416-2243092

Introduction

In a previous article [1], the authors empirically modeled and analyzed heat transfer in a plate heat exchanger (PHE). This article continues that discussion by modeling friction pressure drop in PHEs. A complete thermo-hydraulic analysis is necessary since PHEs are widely deployed in the industry as process heat exchangers. While the surface corrugations on the plates of a PHE can promote turbulent intermixing of the fluid and enhance heat transfer, they also increase the fluid pressure drop. Since any pressure drop has to be compensated by the circulation pump, such pressure losses must be minimized to reduce the pumping power.

Although numerous experimental phase-change studies [2-48] have been reported, the inherent publication bias in those studies needs to be investigated. Studies that repeatedly self-cite or cite a few select articles could be considered biased. Further, the uncertainty estimates reported by each study have to be compared with similar investigations operating under identical normalized test conditions with the same liquid-only Reynolds number Re_{LO}. The homogeneity or consistency in the available data and the validity of the test results in comparison to other studies also need to be investigated. Finally, it needs to be ascertained whether PHEs are more effective than alternatives for condensation and evaporation. Consequently, this article will also report a meta-analysis of the compiled data to check for heterogeneity, bias, and the statistical significance of using PHE condensers and evaporators.

The phase-change mechanisms during condensation and evaporation also alter the fluid pressure drop. For example, for the same liquid-only Reynolds number Re_{LO}, two-phase flows dominated by buoyancy effects tend to have higher frictional pressure drop than the surface tension-dominated flows. Further, the higher-pressure drop was associated with a lower incidence of drop condensation or nucleate boiling, as indicated by the meager Weber number We and the high surface tension energy. A Weber number We significantly less than one makes

bubble formation impossible due to the increased surface tension. Only one article [16] reported flow visualization and detected the various flow regimes during phase-change flows in PHEs.

Consequently, this article attempts to understand the underlying flow physics during phase-change flows in PHEs by modeling the two-phase friction factor f_{TP} in terms of various non-dimensional parameters that model all the relevant forces involved in phase-change processes. Empirical modeling will be deployed using dimensionless parameters such as the Bond number Bd to study local buoyancy. In contrast, parameters such as the Weber number We and Martinelli parameter X will be used to model the drop formation's relevance and estimate the bubble diameter, wetted perimeter, and other hydraulic parameters more accurately.

Currently published correlations [2-3, 6-10, 12-14, 17, 25-27, 29-39, 41-43, 46] are based on limited data and have limited applicability. Given the volume of phase-change experimental data reported with PHEs, it is necessary to periodically update the correlations based on a comprehensive database. This article collected experimental phase-change investigations in PHEs from the last two decades. It developed two universal two-phase friction factor correlations, successfully compared with widely reported correlations, and validated with independent data not used for correlation development.

In conclusion, this article offers an improved understanding of the phase-change flow mechanisms in PHEs. The report also assesses the statistical significance, consistency, and reliability of the data through meta-analysis. Compared to the existing literature, the importance of this article lies in developing more universal correlations as opposed to the current equations with a limited range. The report is also significant because it improves the understanding of buoyancy and surface tension effects during condensation and evaporation. It also provides accurate estimates for the bubble diameter and wetted perimeter and their

contribution to the two-phase pressure drop in terms of the Weber number We and Martinelli parameter X. Finally, the article's uniqueness is in assessing the reliability and consistency of the available data through meta-analysis, a technique currently not used by published investigations.

Sources and filtering

Eleven databases, including the Web of Science, Springer, Google Scholar, Taylor and Francis, IEEE, ASME digital collection, ScienceDirect, SAE Mobilus, Proquest, EBSCO, and SAGE journals, were searched using a keyword search for relevant records. Two hundred fifty-two thousand three hundred eighty shortlisted records were filtered to forty-one two-phase investigations in PHE condensers and evaporators using the selection and exclusion criteria below.

a. Criteria for selection:
    i) Full-length articles must be published in peer-reviewed journals or conference proceedings.
    ii) Articles must be focused on phase change (evaporation or condensation) and not just two-phase (ex: air-water flow) flows.
    iii) Articles must have experimental pressure drop ΔP, pressure gradient dP/dZ, or two-phase friction f_{TP} factor data in PHE condensers or evaporators. Other types of heat exchangers were discarded.
    iv) Articles must provide local or surface-averaged data that varied with the vapor quality x.
b. Criteria for exclusion:
    i) Abstracts, short-length papers, and those without full access were discarded. Articles published in predatory journals and not listed in the Web of Science were discarded.

ii) Experiments in other heat exchangers were discarded.

iii) Experiments without phase-change data (ex, air-liquid flow without phase-change) were discarded.

iv) Experiments without the spatial variation of the pressure drop ΔP or the pressure gradient dP/dZ, or the two-phase friction factor f_{TP} with the vapor quality x were discarded (ex: ΔP or dP/dZ vs. the mass flux G without the vapor quality x were excluded)

v) Articles without numerical uncertainty limits or at least a discussion of experimental uncertainty were discarded.

Figures 1-2 depict the database and records search.

Condensers

Plate heat exchangers are widely used as condensers in the process industry. This section will briefly review the state-of-the-art in PHEs.

Yan et al. [2] conducted condensation pressure drop experiments with R134a in a 6.6 mm hydraulic diameter and a sixty-degree chevron angle PHE condenser. The refrigerant saturation pressure P_{sat} was 7 bar, while the refrigerant mass flux G varied between 60-120 kg/m^2s. The heat flux q" ran from 10 kW/m^2 to 16 kW/m^2 while the vapor quality x ranged from 0.1 to 0.9. At a mass flux of G = 80 kg/m^2s, the frictional pressure drop increased six times as the vapor quality x rose from 0.2 to 0.8. An equivalent Reynolds number Re_{eq}-based correlation was proposed.

Kuo et al. [3] reported friction pressure drop data for condensation of R410A in a 6.6 mm hydraulic diameter and 60° chevron angle vertical PHE condenser. The saturation pressure P_{sat} varied between 1.44-1.95 MPa, while the refrigerant mass flux G ranged from 50 kg/m^2s to 150 kg/m^2s. The heat flux q" ran from 5 kW/m^2 to 20 kW/m^2 while the vapor quality x went

from 0.1 to 0.8. A two-phase friction factor correlation was proposed and successfully compared with their data.

Djordjevic et al. [4] performed condensation pressure drop experiments with R134a in a 3.2 mm hydraulic diameter PHE condenser with a chevron angle $\beta = 63.26°$. The saturation temperature was $T_{sat} = 27.5°C$, while the mass flux G was 50 kg/m^{2}s and 65 kg/m^{2}s. The vapor quality x varied between 0.4 and 0.9, while the heat flux q" ranged from 11.5 kW/m^2 to 17.1 kW/m^2. At a mass flux G = 50 kg/m^{2}s, the friction pressure drop ΔP increased six-fold as the vapor quality x rose from 0.12 to 0.94. No new correlations were reported.

Shon et al. [5] conducted condensation pressure drop experiments with R1233zd(E) in a 3.32 mm hydraulic diameter and a sixty-degree chevron angle PHE condenser. The saturation pressure P_{sat} varied between 2 bar and 3 bar, while the heat flux q" was constant at 2 kW/m^2. The mass flux G was 19.9 kg/m^{2}s and 23.8 kg/m^{2}s, while the vapor quality x ranged from 0.4 to 0.9. A two-phase friction factor correlation was proposed and validated with experimental data.

Soontarapiromsook et al. [6] performed condensation pressure drop experiments with R134a in a 5 mm hydraulic diameter and a sixty-five-degree chevron angle PHE condenser. The saturation temperature T_{sat} was 40°C and 50°C, while the mass flux G was 61 kg/m^{2}s and 89 kg/m^{2}s. The heat flux q" varied between 5-15 kW/m^2, while the vapor quality x went from 0.1 to 0.8. A surface roughness-based two-phase friction factor correlation was proposed and validated with experimental data.

Zhang et al. [7] reported adiabatic condensation pressure drop data in a 3.4 mm hydraulic diameter and a sixty-five-degree chevron angle PHE condenser. The saturation temperature T_{sat} ran from 30°C to 70°C, while the mass flux G was constant at 53 kg/m^{2}s. The

vapor quality x went from 0.3 to 0.9. A two-phase friction factor correlation was proposed and verified with experimental data.

Kwon et al. [8] conducted condensation pressure drop experiments with R1233zd(E) in a 3.88 mm hydraulic diameter and a sixty-degree-chevron angle PHE condenser. The saturation pressure P_{sat} ranged from 2 bar to 3 bar, while the heat flux q" went from 2.5 kW/m^2 to 4.5 kW/m^2. The mass flux G was 19.9 kg/m^{2}s and 23.8 kg/m^{2}s, while the vapor quality x varied between 0.3 and 0.9. A two-phase friction factor correlation was proposed and compared with experimental data.

Park and Kim [9] reported pressure drop data for the condensation of R134a in a 5.6 mm hydraulic diameter and forty-five-degree chevron angle PHE condenser. The saturation temperature T_{sat} varied between 30°C and 40°C while the heat flux q" was 6 kW/m^2 and 8 kW/m^2. The mass flux G went from 40 kg/m^{2}s to 80 kg/m^{2}s while the vapor quality x ran from 0 to 0.9. A two-phase friction factor correlation was proposed in terms of the equivalent Reynolds number Re_{eq} and validated with experimental data.

Park et al. [10] performed condensation pressure drop experiments with R410A in a 5.6 mm hydraulic diameter and a forty-five-degree chevron angle PHE condenser. The saturation temperature T_{sat} varied between 30°C and 40°C, while the heat flux q" ranged from 4 kW/m^2 to 8 kW/m^2. The mass flux G went from 40 kg/m^{2}s to 80 kg/m^{2}s, while the vapor quality varied between 0 and 0.9. A two-phase friction factor correlation in terms of the boiling parameter Bo, the equivalent Reynolds number $Re_{eq,}$ was proposed and compared with experimental data.

Tao et al. [11] conducted adiabatic condensation pressure drop experiments in a 2.99 mm hydraulic diameter and a sixty-three-degree chevron angle PHE condenser. The saturation temperature T_{sat} ranged from 13.4°C to 22.6°C. The mass flux G ran from 21 kg/m^{2}s to 71 kg/m^{2}s, while the vapor quality x went from 0 to 0.6. No correlations were proposed.

Tao and Ferreira [12] reported adiabatic pressure drop data for the condensation of ammonia in a 2.99 mm hydraulic diameter and a sixty-three-degree chevron angle PHE condenser. The saturation pressure P_{sat} was constant at 6.9 bar. The mass flux G ranged from 30 kg/m^{2}s to 71 kg/m^{2}s, while the vapor quality x went from 0 to 0.7. A friction pressure drop model was proposed and validated with experimental data.

Ko et al. [13] performed condensation pressure drop experiments with R124 in two 3.32 mm hydraulic diameter PHE condensers with chevron angles of 30° and 60°. The saturation temperature T_{sat} was 33.74°C and 44.73°C, while the heat flux q" varied between 2.5 kW/m^2 and 4.5 kW/m^2. The mass flux G ranged from 16 kg/m^{2}s to 26 kg/m^{2}s, while the vapor quality x went from 0.3 to 0.9. A two-phase friction factor correlation was proposed in terms of the equivalent Reynolds number Re_{eq} and successfully compared with experimental data.

Jung et al. [14] reported pressure drop data for the condensation of R124 in two 3.88 mm hydraulic diameter PHE condensers of thirty-degree and sixty-degree chevron angles. The saturation pressure P_{sat} was 7.2 bar and 8.2 bar, while the heat flux q" was constant at 2.5 kW/m^2. The mass flux G was steady at 26.5 kg/m^{2}s, while the vapor quality x ranged from 0.5 to 0.9. A new two-phase friction factor correlation was proposed in terms of the equivalent Reynolds number Re_{eq} and was successfully validated with experimental data.

Lee et al. [15] conducted adiabatic condensation pressure drop experiments with R1234ze(E) in a 3.88 mm hydraulic diameter and a sixty-degree chevron angle PHE condenser. The saturation temperature T_{sat} was constant at 15°C. The mass flux G ranged from 50 kg/m^{2}s to 130 kg/m^{2}s, while the vapor quality x went from 0.4 to 0.9. No new correlations were reported.

Wang et al. [16] performed adiabatic condensation pressure drop studies with R365mfc in a 5.195 mm hydraulic diameter and a forty-five-degree chevron angle PHE condenser. The

saturation temperature T_{sat} was constant at 43°C. The mass flux G ranged from 25.35 kg/m^{2}s to 44.74 kg/m^{2}s, while the vapor quality x went from 0.75 to 0.9. No new correlations were reported.

Hu and Ma [17] reported adiabatic pressure drop data for condensing steam and water-ethanol mixture in a 6 mm hydraulic diameter and a sixty-degree chevron angle PHE condenser. The saturation pressure P_{sat} was constant at 0.9 bar, while the mass flux G varied between 5.9 kg/m^{2}s and 14.9 kg/m^{2}s. The vapor quality x ranged from 0.1 to 1.0. A new two-phase friction factor correlation was proposed in terms of the boiling parameter Bo and the equivalent Reynolds number Re_{eq} and was compared with experimental data.

A review of the available condensation studies indicates that although numerous two-phase friction factor predictive correlations [2-3, 6-10, 12-14, 17] exist, they are all based on limited data. Further, most published correlations are based solely on the equivalent Reynolds number Re_{eq}, without additional flow modifiers such as the Martinelli parameter X, the Weber number We, or the Bond number Bd. Although the equivalent Reynolds number does factor in the local vapor quality x and the liquid-vapor density ratio (ρ_L/ρ_V), it doesn't model the impact of buoyancy or drop formation during condensation on the pressure drop. Consequently, this article will propose a more universal condensation friction factor correlation with the appropriate flow modifiers to account for buoyancy, gravitational and surface tension forces, drop formation and wetted perimeter, and the interfacial slip between the liquid and vapor phases during condensation to more accurately model the friction pressure drop.

Table 1 lists all the studies discussed in this section, and each study's corresponding deviation compared to Eq. (1) is presented in the next section.

Regression analysis and correlation development

The compiled condensation data [2-17] was empirically modeled to obtain a two-phase friction factor correlation. Several regression models were deployed, such as linear, non-linear, ANOVA, ANCOVA, and power-law. Power-law regression best fits the data [2-17].

$$f_{TP} = 0.112 Re_{LO}^{-0.34} X^{0.1} Co^{0.66} Bd^{0.92} We^{-0.72} \quad (1)$$

Several dimensionless parameter combinations were attempted to obtain the most accurate correlation. Equation (1) results from the best possible combination of the relevant flow modifiers that most accurately explain the condensation flow phenomena in PHE condensers. As shown in Fig. 3, at a mean bias deviation (MBD) of -5.2% and root-mean-square deviation (RMSD) of 52.1%, and a corresponding R^2 value of 0.65, Eq. (1) fit 15.7% of the data [2-17] within ±10%, 44.6% within ±30%, and 74.6% within ±50%. The Weber number We for all the compiled data [2-17] was less than 1. This indicates that the surface tension forces are dominant, and drop formation is nearly impossible. The negative exponent of the Weber number We also suggest that the pressure drop was not influenced by drop condensation. In contrast, the Bond number Bd was more than one for all the data [2-17]. This suggests that the buoyancy forces dominated the gravitational effects during the condensation process. Since the convection number Co exponent is positive, convective condensation pressure was more significant than drop condensation.

Further, since the convection number Co was much different from one, the interfacial slip between the vapor and liquid phases is substantial, with velocity and momentum mismatches between the two phases at the vapor-liquid interface. Significant liquid droplet entrainment in the vapor flow should be expected, leading to intermixing and increased pressure drop. The negative exponent for the liquid-only Reynolds number indicates that the

two-phase friction factor reduces for turbulent flows. This agrees with the nature of flow in pipes where lower friction factors are measured at higher liquid-only Reynolds numbers.

The collected data [2-17] was compared with widely published correlations. Figure 4 shows the comparison with the Shon et al. [5] correlation. At an MBD of -48.5% and RMSD of 164.6%, the Shon et al. [5] correlation poorly fit the condensation pressure drop data [2-17]. The Shon et al. [5] correlation was based on the equivalent Reynolds number Re_{eq}. Although this parameter includes the local vapor quality and assesses the liquid-vapor fraction correctly in terms of the density ratio (ρ_L/ρ_V), it lacks critical flow modifiers such as the Bond number Bd and the convection number Co. This means that the Shon et al. [5] correlation could not estimate the impact of the buoyancy and slip between the vapor and liquid phases on the condensation pressure drop. This may have resulted in a poor fit. As shown in Fig. 4, the Shon et al. [5] correlation fit 7.5% of the data [5] within ±10%, 15.7% within ±30%, and 27.5% within ±50% at $R^2 = 0.25$.

Comparison with the Zhang et al. [7] correlation is shown in Fig. 5. The Zhang et al. [7] correlation fits 2.1% of the data [2-17] within ±10%, 8.8% within ±30%, and 17.6% within ±50% at $R^2 = 0$. At an MBD of 19.4% and MBD of 514%, the Zhang et al. [7] correlation was a poor fit to the data. Although based on the equivalent Reynolds number Re_{eq} and the homogeneous Weber number We_{homo}, the Zhang et al. [7] correlation lacked the Martinelli parameter and the convection number Co. This means that their correlation did not model the wetted perimeter, liquid fraction, and interfacial slip between the liquid and vapor layers accurately yielding an inaccurate two-phase friction factor. However, the negative exponent of the Weber number in the Zhang et al. [7] equation is similar to Eq. (1), indicating that drop condensation was not the dominant mode of condensation.

The condensation pressure drop data [2-17] was compared with the Ko et al. [13] correlation. As shown in Fig. 6, at an MBD of -398.6% and RSMD of 1157.7%, the Ko et al. [13] correlation fit 14.1% of the data within ±10%, 26.5% within ±30%, and 38.7% within ±50% at $R^2 = 0.11$. The Ko et al. [13] correlation was based on the equivalent Reynolds number Re_{eq}, a geometric parameter Ge that factors in the chevron angle β, and the density ratio (ρ_L/ρ_V). Although the fit is similar to Eq. (1), the MBD is an order of magnitude worse than Eq. (1). In comparison, the RMSD is two orders of magnitude worse than Eq. (1). This could be due to the absence of the Bond number and the convection number which means that the buoyancy and interfacial slip effects were not correctly accounted for in the Ko et al. [13] friction factor correlation. Since the Martinelli parameter was also absent, Ko et al. [13] did not accurately model the wetted perimeter of the liquid and vapor fractions. These issues may have resulted in the poor fit of the data.

Comparison with the Amalfi et al. [18] correlation is shown in Fig. 7. At an MBD of -54.2% and RMSD of 165.7%, the Amalfi et al. [18] correlation fit 7.47% of the condensation pressure drop data [2-17] within ±10%, 20.5% within ±30%, and 33.4% within ±50% at $R^2 = 0.11$. The Amalfi et al. [18] correlation modeled the buoyancy effects accurately by including the Bond number. The negative exponent for the homogeneous Weber number We_{homo} is similar to Eq. (1) and indicates that drop condensation was not the dominant condensation mode. However, the absence of the convection number Co and the Martinelli parameter X may have incorrectly modeled the interfacial slip and the liquid and vapor-wetted perimeters. This may have resulted in a poor fit to the data.

Comparison with the Tao and Ferreira [19] correlation is shown in Fig. 8. At an MBD of -282.1% and RMSD of 796%, the Tao and Ferreira [19] correlation fit 11.3% of the data [2-17] within ±10%, 23.9% within ±30%, and 32.6% within ±50% and $R^2 = 0.58$. The equivalent

Reynolds number Re_{eq}-based correlation [19] also included the Bond number Bd and the Chevron angle β. The reduced pressure P_r-based Tao and Ferreira [19] correlation lacked the Martinelli parameter X and the convection number Co. The Tao and Ferreira correlation [19] did not correctly model the liquid and vapor-wetted perimeters and interfacial slip. This may have resulted in the poor fit of their correlation.

Table 2 summarizes all the correlations presented in this section.

Meta-analysis of condensation in plate heat exchangers

A meta-analysis investigated the garnered data's bias, consistency, homogeneity, and reliability [2-17]. The effect size for each study was based on the mean and standard deviation of the two-phase friction factor f_{TP} and was computed at a 95% confidence interval (CI). Since it was the single most extensive study with two-hundred-and-five data, the Hu and Ma [17] study was chosen as the control group, while the remaining studies [2-16] were selected as the study group. Since all the investigations were conducted under different test conditions, the raw data [2-17] was normalized to the dimensionless control variable $Re_{LO}^{-1.19}X^{-0.12}Co^{0.96}Bd^{0.27}$. This ensured uniformity, and the meta-analysis was performed at a control variable of 0.00026 and the corresponding average liquid-only Reynolds number Re_{LO} of 493. Only the two-phase friction factor f_{TP} data at those values were chosen from each study for meta-analysis. This normalized all the data [2-17] from different test conditions and made the meta-analysis possible.

The Forest plot of the condensation friction factor data, which was derived from the pressure drop data [2-17], is shown in Fig. 9. Significant heterogeneity and inconsistency were detected in the data [2-17] at an I^2 value of 98.8 and Tau^2 value of 16.3. Ideally, I^2 should be less than fifty, and Tau^2 should be zero for consistent and homogeneous data. That means all the studies [2-17] at the identical normalized control variable $Re_{LO}^{-1.19}X^{-0.12}Co^{0.96}Bd^{0.27}$ and

liquid-only Reynolds number Re_{LO} yielded widely different two-phase friction factors while they should have given the same results. This means considerable heterogeneity or inconsistency in the data, which raises not quality but reliability issues.

Except for [7, 9-10], the other studies' effect size does not cross the null line. This means that the remaining data [2-6, 8, 11-17] is statistically significant as the true value of the two-phase friction factor does not lie within the statistical limits. Further, the resultant diamond of the meta-analysis at the bottom of Fig. 9 does not cross the null line and lies between the upper and lower limits of 2.5 and 6.7. These positive limits suggest that PHE condensers are strongly recommended as intervention techniques for minimizing the condensation pressure drop and the two-phase friction factor for condensing flows. The cumulative meta-analysis, the combined result of all the studies, is shown in Fig. 10.

Evaluation of the condensation correlation

Equation (1) was validated with independent data, which were not included in the development. Three independent condensation investigations [20-22] were found and selected for validating Eq. (1). They are listed in Table 3 and are described below.

Han et al. [20] reported condensation pressure drop data for R410A in a 5.1 mm hydraulic diameter PHE condenser with the chevron angle β varying between 20° and 45°. The saturation temperature T_{sat} was 20°C and 30°C, while the heat flux q" went from 4.7 kW/m^2 to 5.3 kW/m^2. The mass flux G was constant at 34 kg/m^{2}s, while the vapor quality x ranged from 0.1 to 0.8. No friction factor correlation was reported.

Muller and Kabelac [21] conducted condensation pressure drop experiments with water and R134a in a 5.2 mm hydraulic diameter PHE condenser with the chevron angle β = 27° and 63°. The saturation temperature T_{sat} was 25.9°C and 112.3°C, while the mass flux G ranged

from 11 kg/m^{2}s to 56 kg/m^{2}s. The heat flux q" was constant at 75.5 kW/m^2 while the vapor quality x was constant at 0.5.

Kwon et al. [22] performed condensation pressure drop experiments with R1233zd(E) in a 3.88 mm hydraulic diameter and a thirty-degree chevron angle PHE condenser. The saturation pressure P_{sat} varied between 2 bar and 3 bar, while the heat flux q" ranged from 1.5 kW/m^2 to 2.5 kW/m^2. The mass flux G was 13.7 kg/m^{2}s and 20 kg/m^{2}s, while the vapor quality x went from 0.2 to 0.9.

As shown in Fig. 11, at an MBD of 2.68% and RMSD of 26%, Eq. (1) fit 30.9% of the evaluation data [20-22] within ±10%, 71.4% within ±30%, and 91.7% within ±50% at R^2 = 0.7. This excellent fit of the independent condensation pressure drop data [20-22] not used for developing Eq. (1) confirms its accuracy.

Table 3 lists all the condensation evaluation data and the corresponding MBD and RMSD for each data set concerning Eq. (1).

Evaporators

Evaporators based on PHEs are also widely used in the process industry. This section lists the state-of-the-art PHE evaporators in the past few decades, followed by empirical modeling, analysis, and meta-analysis. Twenty-four experimental investigations [23-46] were collected for modeling and analysis. Table 4 lists all the studies in this section and the MBD and RMSD of each study compared to Eq. (2), presented in the next section.

Yan et al. [23] reported evaporation pressure drop data for R134a in a 6.6 mm hydraulic diameter and a sixty-degree chevron angle PHE evaporator. The saturation pressure P_{sat} was 6.75 bar and 8 bar, while the heat flux q" was 11 kW/m^2 and 15 kW/m^2. The mass flux G was 55 kg/m^{2}s and 70 kg/m^{2}s, while the vapor quality x ranged from 0.1 to 0.9. No new correlations were reported.

Kim and Lee [24] conducted evaporation pressure drop experiments with R22 and R410A in a 4.3 mm hydraulic diameter PHE evaporator with the chevron angle β varying between 20° and 45°. The saturation temperature T_{sat} went between 5°C and 15°C. While the heat flux q" was constant at 5.5 kW/m^2. No new correlations were reported.

Han et al. [25] performed evaporation pressure drop experiments with R410A in a 5.1 mm hydraulic diameter with the chevron angle β varying between 20° and 45°. The saturation temperature T_{sat} ranged from 5°C to 15°C, while the heat flux q" was constant at 5.5 kW/m^2. The mass flux G was stable at 27 kg/m^{2}s, while the vapor quality x went from 0.1 to 1.0. A new two-phase friction factor correlation was proposed.

Hsieh and Lin [26] reported pressure drop data for the evaporation of R410A in a 6.6 mm hydraulic diameter and a sixty-degree chevron angle PHE evaporator. The saturation pressure P_{sat} was 10.8 bar and 12.5 bar, while the heat flux q" was 10 kW/m^2 and 20 kW/m^2. The mass flux G ranged from 50 kg/m^{2}s to 100 kg/m^{2}s, while the vapor quality x varied between 0.1 and 0.9. A two-phase friction factor correlation was proposed and compared with the data.

Park and Kim [27] conducted evaporation pressure drop experiments with R134a in a 5.6 mm hydraulic diameter and forty-five-degree chevron angle PHE evaporator. The saturation temperature T_{sat} ranged from 0°C to 10°C, while the heat flux q" was 4 kW/m^2 and 6 kW/m^2. The mass flux G ran from 40 kg/m^{2}s to 80 kg/m^{2}s, while the vapor quality went from 0 to 0.9. An equivalent Reynolds number Re_{eq}-based two-phase friction factor correlation was proposed and compared with data.

Taboas et al. [28] performed evaporation pressure drop experiments with an ammonia and water mixture in a 4 mm hydraulic diameter and a thirty-degree chevron angle PHE evaporator. The saturation pressure was 7 bar and 15 bar, while the heat flux q" was 30 kW/m^2

and 35 kW/m^2. The mass flux G ranged from 70 kg/m^{2}s to 140 kg/m^{2}s, while the vapor quality x ranged from 0 to 0.2. No new correlations were proposed.

Khan et al. [29] reported pressure drop data for the evaporation of ammonia in a 4.4 mm hydraulic diameter and a thirty-degree chevron angle PHE evaporator. The saturation temperature T_{sat} varied between -2°C and 25°C, while the heat flux q" was constant at 32.5 kW/m^2. The mass flux G was steady at 5.5 kg/m^{2}s, while the vapor quality x ranged from 0.2 to 0.4. A new two-phase friction factor correlation was proposed in terms of the equivalent Reynolds number Re_{eq} and the critical pressure P_r.

Khan et al. [30] conducted evaporation pressure drop experiments with ammonia in a 4.4 mm hydraulic diameter and a sixty-degree chevron angle PHE evaporator. The saturation temperature T_{sat} went from -2°C to 25°C, while the heat flux q" ranged from 6.9 kW/m^2 to 49.1 kW/m^2. The mass flux G varied between 8 kg/m^{2}s and 27 kg/m^{2}s, while the vapor quality x ranged from 0.1 to 0.5. A new two-phase friction factor correlation was proposed in terms of the equivalent Reynolds number Re_{eq} and the reduced pressure P_r.

Vakili-Farahani et al. [31] performed adiabatic evaporation pressure drop experiments with R245fa in a 1.7 mm hydraulic diameter and a sixty-five-degree chevron angle PHE evaporator. The saturation temperature T_{sat} went from 25°C to 35°C. The mass flux G varied between 10 kg/m^{2}s and 40 kg/m^{2}s while the vapor quality x ranged from 0 to 0.7. A two-phase friction factor correlation was proposed based on the equivalent Reynolds number Re_{eq}.

Lee et al. [32] reported pressure drop experiments for water evaporation in a 5 mm hydraulic diameter and a sixty-degree chevron angle PHE evaporator. The saturation temperature was constant at 103.9°C while the heat flux q" varied between 15 kW/m^2 and 30 kW/m^2. The mass flux G ranged from 14.5 kg/m^{2}s to 24 kg/m^{2}s, while the vapor quality x

went from 0.1 to 0.6. An equivalent Reynolds number Re_{eq}-based two-phase friction factor correlation was proposed.

Khan et al. [33] conducted evaporation experiments with ammonia in a 5.8 mm hydraulic diameter and forty-five-degree chevron angle PHE evaporator. The saturation temperature T_{sat} ranged from -2°C to -25°C, while the heat flux q" went from 21.2 kW/m^2 to 49.1 kW/m^2. The mass flux G was constant at 6.5 kg/m^{2}s, while the vapor quality x varied between 0.5 and 0.9. An equivalent Reynolds number Re_{eq}-based two-phase friction factor correlation was proposed.

Khan et al. [34] performed evaporation pressure drop experiments with ammonia in a 5.8 mm hydraulic diameter and forty-five-degree chevron angle PHE evaporator. The saturation temperature was -2°C and -25°C, while the heat flux q" was 21.2 kW/m^2 and 49.1 kW/m^2. The mass flux G was constant at 6.5 kg/m^{2}s, while the vapor quality x ranged from 0.5 to 0.9. A new two-phase friction factor correlation based on the equivalent Reynolds number Re_{eq} and the reduced pressure P_r was proposed and compared with the data.

Amalfi et al. [35] reported adiabatic pressure drop data for the evaporation of R245fa in a 1.7 mm hydraulic diameter and a sixty-five-degree chevron angle PHE evaporator. The saturation temperature T_{sat} varied between 25°C and 30.5°C. The mass flux G ranged from 15 kg/m^{2}s to 45 kg/m^{2}s, while the vapor quality x went from 0.1 to 0.9. A two-phase friction factor correlation was proposed based on the vapor Reynolds number Re_V.

Desideri et al. [36] reported adiabatic evaporation pressure drop experiments with R245fa and R1233zd in a 3.4 mm hydraulic diameter and a sixty-five-degree chevron angle PHE condenser. The saturation temperature T_{sat} varied between 100-130°C. The mass flux G changed between 68 kg/m^{2}s and 100 kg/m^{2}s, while the vapor quality x went from 0.3 to 0.7. A new friction pressure drop correlation was proposed.

Zhang et al. [37] performed adiabatic evaporation pressure drop experiments with R134a, R124ze, and R1234yf in a 3.4 mm hydraulic diameter and a sixty-five-degree chevron angle PHE evaporator. The saturation temperature T_{sat} ranged from 60°C to 80°C. The mass flux G went from 86 kg/m^{2}s to 137 kg/m^{2}s, while the vapor quality x ranged from 0.5 to 1.0. A new two-phase friction factor correlation was proposed regarding the liquid Reynolds number Re_L and the equivalent Reynolds number Re_{eq}.

Kim et al. [38] reported pressure drop data for the R1234ze(E) evaporation in two 3.37 mm hydraulic diameter PHE evaporators of thirty-degree and sixty-degree chevron angles. The saturation temperature T_{sat} varied between 5°C and 15°C, while the heat flux q" ranged from 6.45 kW/m^2 to 10.4 kW/m^2. The mass flux G went from 21.3 kg/m^{2}s to 58.1 kg/m^{2}s, while the vapor quality x ran from 0.1 to 0.9. An equivalent Reynolds number Re_{eq} and liquid Reynolds number Re_L-based friction factor correlation was proposed.

Lee et al. [39] conducted evaporation pressure drop experiments with R1233zd(E) and R245fa in a 3.88 mm hydraulic diameter and a sixty-degree chevron angle PHE evaporator. The saturation temperature T_{sat} varied between 60°C and 80°C, while the heat flux q" ranged from 6.5 kW/m^2 to 10.4 kW/m^2. The mass flux G went from 32 kg/m^{2}s to 58 kg/m^{2}s, while the vapor quality x ran from 0.1 to 0.9. A two-phase friction factor correlation was proposed in terms of the equivalent Reynolds number Re_{eq}, liquid Reynolds number Re_L, and the liquid Prandtl number Pr_L.

Lee et al. [40] performed evaporation pressure drop experiments with R1234ze(E), R32, and R134a in a 3.88 mm hydraulic diameter and a sixty-degree chevron angle PHE evaporator. The saturation temperature T_{sat} was constant at 15°C, while the heat flux q" was constant at 6.45 kW/m^2. The mass flux G ranged from 32 kg/m^{2}s to 58 kg/m^{2}s, while the vapor quality x went from 0.1 to 0.9. No new friction factor correlations were proposed.

Song et al. [41] reported pressure drop data for the evaporation of R245fa in one 5 mm and a 6 mm hydraulic diameter and sixty-degree chevron angle PHE evaporators. The saturation temperature T_{sat} varied between 60°C and 80°C, while the heat flux q" ranged from 6 kW/m^2 to 9 kW/m^2. The mass flux G ranged from 15 kg/m^{2}s to 30 kg/m^{2}s, while the vapor quality x ranged from 0.1 to 0.8. An equivalent Reynolds number Re_{eq}-based two-phase friction factor correlation was proposed.

Soontarapiromsook et al. [42] conducted evaporation pressure drop experiments with R134a in three PHE evaporators of 5 mm, 10 mm, and 15 mm hydraulic diameters and sixty-five-degree chevron angles. The saturation temperature T_{sat} was constant at 20°C, while the heat flux q" was also constant at 10 kW/m^2. The mass flux G ranged from 67 kg/m^{2}s to 96 kg/m^{2}s, while the vapor quality went from 0.1 to 0.8. An equivalent Reynolds number Re_{eq} and the surface roughness-based equation was proposed.

Jo et al. [43] performed evaporation pressure drop experiments with R1234ze(E) in a 3.315 mm hydraulic diameter and a sixty-degree chevron angle PHE evaporator. The saturation temperature T_{sat} was constant at 15°C, while the heat flux q" was stable at 4.1 kW/m^2. The mass flux G ranged from 20 kg/m^{2}s to 40 kg/m^{2}s, while the vapor quality x went from 0.2 to 0.8. A new two-phase friction factor was proposed in terms of the equivalent Reynolds number Re_{eq} and the liquid Reynolds number Re_L.

Zhang and Haglind [44] reported adiabatic pressure drop data for the evaporation of R134a, R1234ze(E), R236fa, R1233zd(E), propane and isobutane in a 3.4 mm hydraulic diameter and sixty-five-degree chevron angle PHE evaporator. The saturation pressure P_{sat} ranged from 0.165 bar to 27.63 bar. The mass flux G went from 52 kg/m^{2}s to 137 kg/m^{2}s, while the vapor quality x varied between 0.1 and 0.5. No new correlations were reported.

Yang et al. [45] conducted evaporation pressure drop experiments with R32 and R410A in a 3.88 mm hydraulic diameter and a sixty-degree chevron angle PHE evaporator. The saturation temperature T_{sat} was constant at 5°C, while the heat flux q" was constant at 6.45 kW/m^2. The mass flux G ranged from 50 kg/m^{2}s to 90 kg/m^{2}s, while the vapor quality x went from 0.1 to 0.9. No new correlations were reported.

Huang et al. [46] performed evaporation pressure drop experiments with a mixture of R245fa and R134a in a 2 mm hydraulic diameter and a sixty-five-degree chevron angle PHE evaporator. The saturation pressure P_{sat} ranged from 17.9 bar to 27.6 bar, while the heat flux q" went from 15.2 kW/m^2 to 39.7 kW/m^2. The mass flux G varied between 103 kg/m^{2}s and 137 kg/m^{2}s, while the mean vapor quality x went from 0.33 to 0.72. An equivalent Reynolds number Re_{eq} and liquid Reynolds number Re_L-based two-phase friction factor correlation was proposed.

Although numerous predictive two-phase friction factor correlations [25-27, 29-39, 41-43, 46] were proposed for evaporating flows in PHE evaporators, they are based either on the equivalent Reynolds number Re_{eq} or the liquid Reynolds number Re_L. The authors believe they are not complex enough to accurately capture the underlying flow physics. Hence, this article proposes a liquid-only Reynolds number Re_{LO}-based two-phase friction factor correlation modified by suitable flow modifiers such as the Martinelli parameter X, Bond number Bd, Weber number We, convection number Co, reduced pressure $P_{r,}$ and other parameters. These flow modifiers capture the individual flow regimes in the evaporator more accurately by determining if the pool or convective boiling is more significant for the pressure drop. The proposed correlation in the next section also estimates the interfacial slip between the liquid and vapor phases more accurately in terms of the convection number Co.

Regression analysis and correlation development

The collected data [23-46] were correlated using regression tools such as linear, non-linear, ANOVA, ANCOVA, and power-law models. The power-law-based Eq. (2) yielded the best fit to the data.

$$f_{TP} = 0.306 Re_{LO}^{0.18} Bd^{0.52} X^{-0.09} We^{-0.63} Co^{0.16} Bo^{0.02} P_r^{-0.48} \left(\frac{\rho_L}{\rho_V}\right)^{-1.24} \left(\frac{\mu_L}{\mu_V}\right) \qquad (2)$$

Like Eq. (1), the best combination of flow modifiers was included in Eq. (2) to yield the best possible fit and explain the flow physics satisfactorily. As shown in Fig. 12, at an MBD of -15.3% and RMSD of 64.5%, Eq. (2) fit 14.3% of the data [23-46] within ±10%, 42.7% within ±30%, and 64.9% within ±50%. The corresponding R^2 value was 0.71. The Bond number Bd for all the studies [23-46] was more than one. This suggests that the buoyancy effects dominated the surface tension forces during evaporation and subsequent pressure drop in the PHE evaporator. Further, the positive exponent for the convection number Co and a density ratio (ρ_L/ρ_V) of more than one indicates significant relative motion between the liquid and vapor phases at the interface during evaporation in the PHE. Vapor bubble entrainment into the evaporation film may have increased the pressure drop more than direct convective evaporation. The Weber number We for all the data [23-46] was much less than one, indicating the surface tension energy was very high, making pool boiling impossible. This means that convective and film boiling were predominant during evaporation in the PHE.

Equation (2) was compared with several widely reported correlations. Comparison with the Khan et al. [30] correlation is shown in Fig. 13. At an MBD of -5812.8% and RMSD of 8128.9%, the Khan et al. [30] correlation fit a mere 0.1% of the data [23-46] within ±50% at $R^2 = 0.27$. The Khan et al. [30] equation was based on the equivalent Reynolds number Re_{eq} and the reduced pressure P_r. The equivalent Reynolds number Re_{eq} incorporates the vapor quality x and the density ratio (ρ_L/ρ_V). However, the lack of crucial flow modifiers such as the

Bond number Bd, convection number Co, and the Weber number means that the correlation could not accurately estimate the buoyancy, surface tension effects, interfacial slip, and surface tension forces. This may have resulted in a poor fit.

The Song et al. [41] correlation was compared with Eq. (2). As shown in Fig. 14, at an MBD of -8550% and RMSD of 36,440%, the Song et al. [41] correlation fit 0.8% of the data [23-46] within ±10%, 2.5% within ±30%, and 2.9% within ±50% at $R^2 = 0.15$. The Song et al. [41] equation is a simple correlation based solely on the equivalent Reynolds number Re_{eq}. Although their equation involves the local vapor quality and the density ratio (ρ_L/ρ_V), no relevant flow modifiers such as the Weber number We, Bond number Bd, or the Martinelli parameter X were incorporated. The Song et al. [41] correlation did not accurately model the wetted perimeter, bubble diameter, buoyancy, surface tension, and gravity effects during evaporation. This may have resulted in an inaccurate estimate of the evaporation pressure drop.

Comparison with the Soontarapiromsook et al. [42] correlation is shown in Fig. 15. At an MBD of -175.5% and RMSD of 1001%, the Soontarapiromsook et al. [42] correlation fit 9.81% of the data [23-46] within ±10%, 26.8% within ±30%, and 39.7% within ±50% at $R^2 = 0.11$. Although the fit is similar to Eq. (2), the MBD and RMSD are several orders of magnitude worse. Although the Soontarapiromsook et al. [42] correlation incorporates surface roughness, the equivalent Reynolds number Re_{eq} isn't sufficient to accurately model the buoyancy, surface tension, and gravitational effects.

The Huang et al. [46] correlation is shown in Fig. 16. At an MBD of -140% and RMSD of 980.5%, the Huang et al. [46] correlation fit 3.9% of the data [23-46] within ±10%, 17.8% within ±30%, and 37.5% within ±50% at $R^2 = 0.19$. Although the fit is similar to Eq. (2), the Huang et al. [46] correlation is based only on the equivalent Reynolds number Re_{eq} and the liquid Reynolds number Re_L. Several flow phenomena, such as vapor bubble formation or the

absence of it, slug, annular or bubbly flow, and their impact on the pressure drop were not incorporated into their equation in terms of the Weber number We, Martinelli parameter X, and Bond number Bd. This may have resulted in a poor fit.

Comparison with the Huang et al. [47] equation is shown in Fig. 17. At an MBD of -1267.7% and RMSD of 2289.3%, the Huang et al. [47] correlation fit 0.5% of the data [23-46] within ±10%, 1.7% within ±30%, and 3.6% within ±50% at $R^2 = 0.17$. The Huang et al. [47] correlation is based on the two-phase Reynolds number Re_{TP} and the geometrical parameter F_{RF}, which considers the chevron angle β. Their correlation considers the density ratio (ρ_L/ρ_V) and the vapor quality and would have accurately predicted the slip velocity at the vapor-liquid interface. However, the lack of flow modifiers such as the Weber number We, the Bond number Bd, and the Martinelli parameter X means that bubble formation, buoyancy, and surface tension effects were not correctly incorporated into the pressure drop model. This may have resulted in a poor fit to the data [23-46].

Table 5 lists all the correlations cited in this section.

Meta-analysis of evaporation in plate heat exchangers

A meta-analysis of the evaporation pressure drop data [23-46] was also conducted to determine the data's bias, reliability, homogeneity, and consistency. To normalize the different test conditions and variables involved in the studies [23-46], the non-dimensional control variable was set as $Re_{LO}^{0.18} Bd^{0.52} X^{-0.09} We^{-0.63} Co^{0.16} Bo^{0.02} P_r^{-0.48} \left(\frac{\rho_L}{\rho_V}\right)^{-1.24} \left(\frac{\mu_L}{\mu_V}\right)$. Only the two-phase friction factors at the control variable of 2.46 and an average liquid-only Reynolds number Re_{LO} of 791 were chosen from each study [23-46] for meta-analysis. This ensured parametric similarity and normalization of the various studies conducted at different test conditions.

Multiple friction factor data at the same control variable were averaged, and the number of samples was included in the computations. The difference in the mean values of friction factors and the standard deviation were computed from the raw data [23-46] at 95% CI. As shown in the Forest plot in Fig. 18, the resultant effect size of the meta-analysis demonstrated as a diamond at the bottom of the figure crosses the null line. This means that the true mean of the computed two-phase friction factor f_{TP} lies within the 95% CI bands. Hence, the meta-analysis is statistically insignificant and inconclusive. The current practice of using PHE evaporators for lowering the refrigerant side pressure drop in the process industry can continue.

Considerable heterogeneity and inconsistency were detected in the compiled data [23-46]. An I^2 value of 93.3 and a Tau^2 value of 9.72 indicates a significant inconsistency in the data. For data to be homogeneous and consistent, the I^2 value should be less than fifty, while the Tau^2 value should be zero. This means that the friction factor data from different studies [23-46] compiled at the same similarity or control variable and liquid-only Reynolds number Re_{LO} were significantly different when they should have been similar. Although the investigation test conditions were [23-46] considerably different, they were all reduced to the same non-dimensional similarity or control variable and the liquid-only Reynolds number Re_{LO} and should have yielded similar results. This raises reliability, but not accuracy, issues about the compiled data [23-46]. Although inconclusive, the final effect size diamond tends towards the Zhang and Haglind [44] study. This means out of all the compiled data [23-46], the Zhang and Haglind [44] data is more reliable. However, this does not mean the rest of the data is inaccurate. It only means that among the compiled studies [23-46], the Zhang and Haglind [44] pressure drop and friction factor data are more reliable than others. The cumulative meta-analysis is shown in Fig. 19.

Validation of the correlation for evaporation

To verify its accuracy and reliability, Eq. (2) was tested with evaporation pressure drop data [35 and 48]. The widely reported Longo et al. [48] study was the only independent data that could be found for evaluating Eq. (2). This eliminated data bias as using all the development data [23-46] would have yielded the exact fit as in Fig. 3 and would have artificially made it look better. Hence, at least one independent data set [48] was used for validation to ensure an unbiased and independent corroboration of the accuracy of Eq. (2). Table 6 lists the evaluation data and the MBD and RSMD for each data set in comparison to Eq. (2).

Amalfi et al. [35] reported adiabatic pressure drop data for the evaporation of R245fa in a 1.7 mm hydraulic diameter and a sixty-five-degree chevron angle PHE evaporator. The saturation temperature T_{sat} varied between 25°C and 30.5°C. The mass flux G ranged from 15 kg/m^{2}s to 45 kg/m^{2}s, while the vapor quality went from 0.1 to 0.9. A local two-phase Fanning friction factor correlation was proposed in terms of the vapor Reynolds number Re_V. This data was one of the most widely reported and was included to enhance the volume of the evaluation data.

Longo et al. [48] reported pressure drop data for the evaporation of R1234ze(Z) and R1233zd(E) in a 4 mm hydraulic diameter and a sixty-five-degree chevron angle PHE evaporator. The saturation temperature T_{sat} varied between 30°C and 40°C, while the heat flux q" was constant at 12.15 kW/m^2. The mass flux G went from 5.6 kg/m^{2}s to 25.6 kg/m^{2}s, while the vapor quality x was 0.51 and 0.61. No new correlations were reported. This independent data set was not used to develop Eq. (2).

As shown in Fig. 20, at an MBD of 16.3% and RSMD of 33.5%, Eq. (2) fit 22.7% of the evaluation data [35 and 48] within ±10%, 58% within ±30%, and 89.8% within ±50% at $R^2 = 0.79$. This excellent fit corroborates the accuracy and reliability of Eq. (2).

Conclusions

1. Two-phase friction factor correlations that are patterned after the traditional single-phase friction factor correlations in terms of the equivalent Reynolds number Re_{eq} or the two-phase Reynolds number Re_{TP} were generally poor fits for the condensation pressure drop data [2-17], and the evaporation pressure drop data [23-46]. Such traditional models do not fully account for the buoyancy, convection, surface tension, and gravitational effects during phase-change pressure drop. More detailed local and flow-regime specific (ex, slug, bubbly, annular, etc., flow regimes) pressure drop experiments focused exclusively on measuring the interfacial slip, buoyancy, surface tension, and gravitational effects are necessary for estimating their impact on the friction pressure drop.
2. Except for the Zhang et al. [7] correlation, which deployed a homogeneous Weber number $We_{homo,}$ and the Amalfi et al. [18] correlation, which deployed both the Bond number Bd and the homogeneous Weber number We_{homo}, all the other correlations were based on the equivalent Reynolds number Re_{eq} and the liquid Reynolds number Re_L. This method of modeling the two-phase friction factor correlations after single-phase flow correlations without phase-change modifiers resulted in poor fits for such correlations.
3. Drop and bubble formation may have been minimal or impossible for all the studies [2-46] as the Weber numbers We were much less than one. Due to the dominance of surface tension, drop condensation, and nucleate boiling were either negligible or impossible due to the high surface tension energy, which may have made drop or bubble formation impossible. Weber numbers above one indicate low surface tension fluids that promote drop condensation or nucleate boiling. The use of low-surface tension fluids is encouraged for better thermo-hydraulic performance.

4. The Bond number Bd for all the studies [2-46] was greater than one, suggesting that buoyancy effects dominated gravitational effects during condensation and evaporation pressure drop.
5. The convection number Co and the density ratio (ρ_L/ρ_V) were much different than one for all the studies [2-46]. A density ratio of one would indicate momentum and force balance at the liquid-vapor interface. However, since both the convection number Co and the density ratio were significantly different than one, considerable momentum imbalance should have occurred at the liquid-vapor interface in the condensing and evaporating flows, leading to a slip between the phases. This may have increased the pressure drop. It is recommended to use refrigerants with near identical liquid and vapor phase densities to eliminate the interfacial slip and reduce the pressure drop.
6. At an MBD of -5.2% and RMSD of 52.1%, Eq. (1) fit 15.7% of the data [2-17] within ±10%, 44.6% within ±30%, and 74.6% within ±50%. Surface tension, buoyancy, and interfacial slip effects were dominant in the condensation pressure drop. The reliability of Eq. (1) was confirmed by comparing it with independent data [20-22]. At an MBD of 2.68% and RMSD of 26%, Eq. (1) fit 30.9% of the evaluation data [20-22] within ±10%, 71.4% within ±30%, and 91.7% within ±50%. Similarly, at an MBD of -15.3% and RMSD of 64.5%, Eq. (2) fit 14.3% of the data [23-46] within ±10%, 42.7% within ±30%, and 64.9% within ±50%. Film boiling was most likely the dominant evaporation mode, with pool boiling being the least significant. Equation (2) was validated with one widely reported data set [35] and one independent data set [48]. At an MBD of 16.3% and RSMD of 33.5%, Eq. (2) fit 22.7% of the evaluation data [35 and 48] within ±10%, 58% within ±30%, and 89.8% within ±50%.
7. Meta-analysis indicated considerable heterogeneity and inconsistency in the condensation [2-17] and evaporation [23-46] pressure drop data, raising reliability, but

not quality, issues. The analysis strongly recommended PHE condensers for reducing the refrigerant condensation friction pressure drop and pump duty. Meta-analysis was inconclusive for evaporators, and the current practice of using PHEs should continue.

Nomenclature

A	Area of cross section (m^2)
A_P	Plate area (m^2)
ANOVA	Analysis of variance
ANCOVA	Analysis of Covariance
Bo	Boiling parameter $\left(\frac{q"}{Gi_{fg}}\right)$
Bd	Bond number $\left(\frac{g(\rho_L-\rho_v)d_h^2}{\sigma}\right)$
CI	Confidence interval
C_L	Liquid phase Martinelli constant
Co	Convection number $\left(\frac{\rho_v}{\rho_L}\right)^{0.5}\left(\frac{1-x}{x}\right)^{0.8}$
C_v	Vapor phase Martinelli constant
d_h	Hydraulic diameter (m)
exp	Experimental value
f_{TP}	Two-phase Fanning friction factor ($f_{TP} = \frac{\Delta P\ \rho_m d_h}{2G^2L}$)
F_{RF}	Geometric parameter
g	Gravitational acceleration (9.81 m/s^2)
G	Mass velocity $\left(\frac{\dot{m}}{A}\right)$ (kg/m^2s)
G_{eq}	Equivalent mass flux $G(1-x)+x\left(\frac{\rho_L}{\rho_v}\right)^{0.5}$ (kg/m^2s)

Ge	Geometric parameter $\left(\frac{\beta}{180}\right)\pi$
i_{fg}	Latent heat of vaporization (kJ/Kg K)
I^2	Heterogeneity index (I-squared)
L	Port-to-port length of the PHE (m)
$\dot{m}$	Mass flow rate (kg/s)
MBD	Mean bias deviation $\frac{1}{N}\sum\left(\frac{exp-pred}{exp}\right)$
N	Count; sample size; the number of data
P_{crit}	Critical pressure (Pa)
P_r	Reduced pressure $\left(\frac{P_{sat}}{P_{crit}}\right)$
P_{sat}	Saturation pressure
ΔP	Pressure drop (Pa)
$\frac{dP}{dZ}$	Pressure gradient (Pa/m)
PHE	Plate heat exchanger
Pr_L	Liquid Prandtl number
pred	Predicted value
q”	Heat flux (W/m^2)
R	$\frac{\beta}{30°}$
Re_{eq}	$\left(\frac{G_{eq}d_h}{\mu_L}\right)$

Re_L	Liquid Reynolds number $\left(\frac{G d_h}{\mu_L}\right)$
Re_{LO}	Liquid-only Reynolds number $\left(\frac{G(1-x) d_h}{\mu_L}\right)$
Re_{TP}	$\left(\frac{G d_h}{\mu_{TP}}\right)$
Re_V	Vapor Reynolds number $\left(\frac{G d_h}{\mu_V}\right)$
RMSD	Root mean square deviation $\sqrt{\frac{1}{N}\sum\left\{\left(\frac{exp-pred}{exp}\right)^2\right\}}$
R^2	Coefficient of determination
T_{sat}	Saturation temperature (K)
Tau^2	Absolute value of true variance (Heterogeneity)
We	Weber number $\left(\frac{G^2 d_h}{\sigma \rho_L}\right)$
We_{homo}	Homogeneous Weber number $\left(\frac{G^2 d_h}{\rho_m \sigma}\right)$
x	Vapor quality

Greek Symbols

β	Chevron angle (°)
ε	Surface roughness (μm)
X	$\left(\left(\frac{1-x}{x}\right)\left(\frac{\rho_V}{\rho_L}\right)\left(\frac{\mu_L}{\mu_V}\right)\right)^{\frac{1}{2}}$ (for $Re_{LO} < 2000$ and $Re_V < 2000$)
	$\sqrt{Re_V^{-0.8}\left(\frac{C_L}{C_V}\right)\left(\frac{\dot{m}_L}{\dot{m}_V}\right)\left(\frac{\rho_L}{\rho_V}\right)\left(\frac{\mu_L}{\mu_V}\right)}$ (for $Re_{LO} < 1000$ and $Re_V > 2000$, and $Re_{LO} > 2000$

and $Re_{LO} < 1000$. $C_L = 16$ and $C_V = 0.046$ for $Re_{LO} < 1000$ and $Re_v > 2000$; $C_L = 0.046$ and $C_V = 16$ for $Re_{LO} > 2000$ and $Re_v < 1000$; $\dot{m}_L = G(1-x)A$ and $\dot{m}_v = GxA$)

$\left(\frac{1-x}{x}\right)^{0.8}\left(\frac{\rho_v}{\rho_L}\right)^{0.5}\left(\frac{\mu_L}{\mu_V}\right)^{0.1}$ (for $Re_{LO} > 2000$ and $Re_V > 2000$)

μ	Dynamic viscosity (Pa.s)
μ_{TP}	Two-phase dynamic viscosity $\rho_m\left(x\left(\frac{\mu_V}{\rho_V}\right)+(1-x)\left(\frac{\mu_L}{\rho_L}\right)\right)$
ρ	Density (kg/m^3)
ρ_m	Mean density (kg/m^3) $\left[\left(\frac{1-x}{\rho_L}\right)+\left(\frac{x}{\rho_V}\right)\right]^{-1}$
σ	Surface tension (N/m)

Subscripts

eq	Equivalent
exp	Experimental value
h	Hydraulic parameter
homo	Homogeneous model-based parameter
L	Liquid
LO	Liquid-only
m	mean value
max	maximum value

out	Outlet value
pred	Predicted value
sat	Saturated state
TP	Two-phase flow parameter
V	Vapor

Acknowledgments

The authors thank the University of Pretoria and the Vellore Institute of Technology for the research resources. No conflicts of interest are reported.

References

[1] Y. Mukkamala and J. Dirker, “Empirical modeling and meta-analysis of heat transfer in plate heat exchangers,” *Heat Transf. Eng.,* vol. 45, no. 16, Oct. 2023. 10.1080/01457632.2023.2260524

[2] Y.Y. Yan, H.C. Lio, and T.F. Lin, "Condensation heat transfer and pressure drop of refrigerant R-134a in a plate heat exchanger", *Int. J. Heat Mass Transf.,* vol. 42, no.6, pp. 993-1006, Mar. 1999. DOI: 10.1016/S0017-9310(98)00217-8.

[3] W.S. Kuo, Y.M. Lie, Y.Y. Hsieh, and T.F. Lin, "Condensation heat transfer and pressure drop of refrigerant R-410A flow in a vertical plate heat exchanger", *Int. J. Heat Mass Transf.,* vol. 48, no. 25-26, pp. 5205-5220, Dec. 2005. DOI: 10.1016/j.ijheatmasstransfer.2005.07.023.

[4] E.M. Djordjevic, S. Kabelac, and S. Serbanovic, "Heat transfer coefficient and pressure drop during refrigerant R-134a condensation in a plate heat exchanger", *Chem. Pap.,* vol. 62, no. 1, pp. 78-85, Feb. 2008. DOI: 10.2478/s11696-007-0082-8.

[5] B.H. Shon, C.W. Jung, O.J. Kwon, C.K. Choi, and Y.T. Kang, "Characteristics on condensation heat transfer and pressure drop for a low GWP refrigerant in brazed plate heat exchanger," *Int. J. Heat Mass Transf.,* vol. 122, pp. 1272-1282, Jul. 2018. DOI: 10.1016/j.ijheatmasstransfer.2018.02.077.

[6] J. Soontarapiromsook, O. Mahian, A.S. Dalkilic, and S. Wongwises, "Effect of surface roughness on the condensation of R-134a in vertical chevron gasketed plate heat exchangers", *Exp. Therm. Fluid Sci.,* vol. 91, pp. 54-63, Feb. 2018. DOI: 10.1016/j.expthermflusci.2017.09.015.

[7] J. Zhang, M.R. Kaern, T. Ommen, B. Elmegaard, and F. Haglind, "Condensation heat transfer and pressure drop characteristics of R134a, R1234ze(E), R245fa, and R1233zd(E) in

a plate heat exchanger", *Int. J. Heat Mass Transf.*, vol. 128, pp. 136-149, Jan. 2019. DOI: 10.1016/j.ijheatmasstransfer.2018.08.124.

[8] O.J. Kwon, B.H. Shon, and Y.T. Kang, "Experimental investigation on condensation heat transfer and pressure drop of a low GWP refrigerant R-1233zd(E) in a plate heat exchanger", *Int. J. Heat Mass Transf.*, vol. 131, pp. 1009-1021, Mar. 2019. DOI: 10.1016/j.ijheatmasstransfer.2018.11.114.

[9] J.H. Park and Y.S. Kim, "Condensation heat transfer and pressure drop of R134a in the oblong shell and plate heat exchanger", *Int. J. Air-Cond. Refrig*., vol. 12, no. 3, pp. 158-167, 2004.

[10] J.H. Park, Y.C.H. Kwon, and Y.S. Kim, "Experimental study on R-410A condensation heat transfer and pressure drop characteristics in oblong shell and plate heat exchanger", presented at the Int. Refrig. and Air-Cond. Conf., Purdue, USA, article no. R061, 8 pages, Jul. 12-15, 2004.

[11] X. Tao, E. Dahlgren, M. Leichsenring, and C.A.I. Ferreira, "NH_3 condensation in a plate heat exchanger: Experimental investigation on flow patterns, heat transfer and frictional pressure drop", *Int. J. Heat Mass Transf*., vol. 151, article no. 119374, Apr. 2020. DOI: 10.1016/j.ijheatmasstransfer.2020.119374.

[12] X. Tao and C.A.I. Ferreira, "NH_3 condensation in a plate heat exchanger: Flow pattern-based models of heat transfer and friction pressure drop", *Int. J. Heat Mass Transf.*, vol. 154, article no. 119774, Jun. 2020. DOI: 10.1016/j.ijheatmasstransfer.2020.119774.

[13] Y.M. Ko, J.H. Jung, S. Sohn, C.H. Song, and Y.T. Kang, "Condensation heat transfer performance and integrated correlations of low GWP refrigerants in plate heat exchangers," *Int. J. Heat Mass Transf.*, vol. 177, article no 121519, 13 pages, Oct. 2021. DOI: 10.1016/j.ijheatmasstransfer.2021.121519.

[14] J.H. Jung, Y.M. Ko, and Y.T. Kang, "Condensation heat transfer characteristics and energy conversion performance analysis for low GWP refrigerants in plate heat exchangers," *Int. J. Heat Mass Transf.*, vol. 166, article no. 120727, 12 pages, Feb. 2021. DOI: 10.1016/j.ijheatmasstransfer.2020.120727.

[15] D.C. Lee, S. Yun, J.Y. Choi, and Y. Kim, "Flow patterns and heat transfer characteristics of R-1234ze(E) for downward condensation in a plate heat exchanger", *Int. J. Heat Mass Transf.*, vol. 175, article no. 121373, 16 pages, Aug. 2021. DOI: 10.1016/j.ijheatmasstransfer.2021.121373.

[16] R. Wang, Y. Zhang, W. Li, and S. Kabelac, "Flow pattern, heat transfer and frictional pressure drop investigation of R365mfc condensation in a micro-structured corrugated gap with mixed angles", *Appl. Therm. Eng.*, vol. 201, part B, article no. 117812, 13 pages, Jan. 2022. DOI: 10.1016/j.applthermaleng.2021.117812.

[17] S. Hu and X. Ma, "Experimental study of pressure drop during water-ethanol condensation in a vertical plate heat exchanger," *Heat Mass Transf.*, vol. 58, no. 4, pp. 1289-1302, Aug. 2022. DOI: 10.1007/s00231-022-03175-5.

[18] R.L. Amalfi, F. Vakili-Farahani, and J.R. Thome, "Flow boiling and frictional pressure gradients in plate heat exchangers. Part 2: Comparison of literature methods to database and new prediction methods", *Int. J Refrig.*, vol. 61, pp. 185-203. Jan. 2016. DOI: 10.1016/j.ijrefrig.2015.07.009.

[19] X. Tao and C.A.I. Ferreira, "Heat transfer and frictional pressure drop during condensation in plate heat exchangers: Assessment of correlations and a new method," *Int. J Heat Mass Transf.*, vol. 135, pp. 996-1012, Jun. 2019. DOI: 10.1016/j.ijheatmasstransfer.2019.01.132.

[20] D.H. Han, K.J. Lee, and Y.H. Kim, "The characteristics of condensation in brazed plate heat exchangers with different chevron angles," *J. Korean Phy. Soc*., vol. 43, no.1, pp. 66-73, Jul. 2003.

[21] A. Muller and S. Kabelac, "The experimental determination of heat transfer and pressure drop during condensation in a plate heat exchanger with corrugated plates," *WIT Trans. Eng. Sci*., vol. 83, pp. 337-349, Jul. 2014. DOI: 10.2495/HT140301.

[22] O.J. Kwon, J.H. Jung, and Y.T. Kang, "Development of experimental Nusselt number and friction factor correlations for condensation of R-1233zd(E) in plate heat exchangers", *Int. J. Heat Mass Transf.*, vol. 158, article no. 120008, 15 pages, Sep. 2020. DOI: 10.1016/j.ijheatmasstransfer.2020.120008.

[23] Y.Y. Yan, T.F. Lin, and B.C. Yang, "Evaporation heat transfer and pressure drop of refrigerant R134a in a plate heat exchanger", presented at the ASME ASIA '97 Congr., Singapore, Oct. 2, 1997.

[24] Y.H. Kim and K.J. Lee, "An experimental study on evaporation heat transfer and pressure drop in plated heat exchangers with different chevron angles," *Trans. Korean Soc. Mech. Eng.* Part B, vol. 26, no. 2, pp. 269-277, Feb. 2002. DOI: 10.3795/ksme-b.2002.26.2.269.

[25] D.H. Han, K.J. Lee, and Y.H. Kim, "Experiments on the characteristics of evaporation of R410A in brazed plate heat exchangers with different geometric configurations", *Appl. Therm. Eng*., vol. 23, no. 10, pp. 1209-1225, Jul. 2003. DOI: 10.1016/S1359-4311(03)00061-9.

[26] Y.Y. Hsieh and T.F. Lin, "Evaporation heat transfer and pressure drop of refrigerant R-410A flow in a vertical plate heat exchanger", *J. Heat Transf.*, vol. 125, no. 5, pp. 852-857, Oct. 2003. DOI: 10.1115/1.1518498.

[27] J.H. Park and Y.S. Kim, "Evaporation heat transfer and pressure drop characteristics of R-134a in the oblong shell and plate heat exchanger", *KSME Int. J.*, vol. 18, no. 12, pp. 2284-2293, 2004.

[28] F. Taboas, M. Valles, M. Bourouis, and A. Coronas, "Flow boiling heat transfer of ammonia/water mixture in a plate heat exchanger," *Int. J. Refrig.*, vol. 33, no. 4, pp. 695-705, Jun. 2010. DOI: 10.1016/j.ijrefrig.2009.12.005.

[29] M.S. Khan, T.S. Khan, M.C. Chyu, and Z.H. Ayub, "Experimental investigation of evaporation heat transfer and pressure drop of ammonia in a 30° chevron plate heat exchanger", *Int. J. Refrig.*, vol. 35, no. 6, pp. 1757-1765, Sep. 2012. DOI: 10.1016/j.ijrefrig.2012.05.019.

[30] T.S. Khan, M.S. Khan, M.C. Chyu, and Z.H. Ayub, "Experimental investigation of evaporation heat transfer and pressure drop in a 60° chevron plate heat exchanger", *Int. J. Refrig.*, vol. 35, no. 2, pp. 336-348, Mar. 2012. DOI: 10.1016/j.ijrefrig.2011.10.018.

[31] F. Vakili-Farahani, R.L. Amalfi, and J.R. Thome, "Two-phase flow and boiling of R245fa in a 1 mm pressing depth plate heat exchanger - Part I: Adiabatic pressure drop", *Interfacial Phenom. Heat Transf.*, vol. 2, no. 4, pp. 325-342, 2014. DOI: 10.1615/InterfacPhenomHeatTransfer.2015012027.

[32] E. Lee, H. Kang, and Y. Kim, "Flow boiling heat transfer and pressure drop of water in a plate heat exchanger with corrugated channels at low mass flux conditions," *Int. J. Heat Mass Transf.*, vol. 77, pp. 37-45, Oct. 2014. DOI: 10.1016/j.ijheatmasstransfer.2014.05.019.

[33] M.S. Khan, T.S. Khan, M.C. Chyu, and Z.H. Ayub, "Evaporation heat transfer and pressure drop of ammonia in a mixed configuration chevron plate heat exchanger," *Int. J. Refrig.*, vol. 41, pp. 92-102, May 2014. DOI: 10.1016/j.ijrefrig.2013.12.015.

[34] T.S. Khan, M.S. Khan, M.C. Chyu, and Z.H. Ayub, "Ammonia evaporation in a mixed configuration chevron plate heat exchanger with and without miscible oil," *Int. J. Refrig*., vol. 51, pp. 120-134, Mar. 2015. DOI: 10.1016/j.ijrefrig.2014.12.002.

[35] R.L. Amalfi, J.R. Thome, V. Solotych, and J. Kim, "High resolution local heat transfer and pressure drop infrared measurements of two-phase flow of R245fa within a compact plate heat exchanger", *Int. J. Heat Mass Transf.*, vol. 103, pp. 791-806, Dec. 2016. DOI: 10.1016/j.ijheatmasstransfer.2016.07.060.

[36] A. Desideri et al., "An experimental analysis of flow boiling and pressure drop in a brazed plate heat exchanger for organic Rankine cycle power systems," *Int. J. Heat Mass Transf.*, vol. 113, pp. 6-21, Oct. 2017. DOI: 10.1016/j.ijheatmasstransfer.2017.05.063.

[37] J. Zhang et al., "Flow boiling heat transfer and pressure drop characteristics of R134a, R1234yf, and R1234ze in a plate heat exchanger for organic Rankine cycle units", *Int. J. Heat Mass Transf*., vol. 108, Part B, pp. 1787-1801, May 2017. DOI: 10.1016/j.ijheatmasstransfer.2017.01.026.

[38] D. Kim, D.C. Lee, D.S. Jang, Y. Jeon, and Y. Kim, "Comparative evaluation of flow boiling heat transfer characteristics of R-1234ze(E) and R-134a in plate heat exchangers with different chevron angles", *Appl. Therm. Eng.*, vol. 132, pp. 719-729, Mar. 2018. DOI: 10.1016/j.applthermaleng.2018.01.019.

[39] D.C. Lee, D. Kim, S. Park, J. Lim, and Y. Kim, "Evaporation heat transfer coefficient and pressure drop of R-1233zd(E) in a brazed plate heat exchanger", *Appl. Therm. Eng*., vol. 130, pp. 1147-1155, Feb. 2018. DOI: 10.1016/j.applthermaleng.2017.11.088.

[40] D.C. Lee, D. Kim, W. Cho, and Y. Kim, "Evaporation heat transfer and pressure drop characteristics of R1234Ze(E)/R32 as a function of composition ratio in a brazed plate heat

exchanger", *Int. J. Heat Mass Transf.*, vol. 140, pp. 216-226, Sep. 2019. DOI: 10.1016/j.ijheatmasstransfer.2019.06.004.

[41] K.S. Song, S. Yun, D.C Lee, K. Kim, and Y. Kim, "Evaporation heat transfer characteristics of R-245fa in a shell and plate heat exchanger for very-high-temperature heat pumps", *Int. J. Heat Mass Transf.*, vol. 151, article no. 119408, 10 pages, Apr. 2020. DOI: 10.1016/j.ijheatmasstransfer.2020.119408.

[42] J. Soontarapiromsook et al., "Experimental investigation on two-phase heat transfer of R134a during vaporization in a plate heat exchanger with rough surface", *Int. J. Heat Mass Transf.*, vol. 160, article 120221, 10 pages, Oct. 2020. DOI: 10.1016/j.ijheatmasstransfer.2020.120221.

[43] C.U. Jo, D.C. Lee, H.J. Chung, Y. Kang, and Y. Kim, "Comparative evaluation of the evaporation heat transfer characteristics of a low-GWP-refrigerant R-1234Ze(E) between shell-and-plate and plate heat exchangers", *Int. J. Heat Mass Transf.*, vol. 153, article no. 119598, 10 pages, Jun. 2020. DOI: 10.1016/j.ijheatmasstransfer.2020.119598.

[44] J. Zhang and F. Haglind, "Experimental analysis of high temperature flow boiling heat transfer and pressure drop in a plate heat exchanger," *Appl. Therm. Eng.*, vol. 196, article no. 117269, 14 pages, Sep. 2021. DOI: 10.1016/j.applthermaleng.2021.117269.

[45] J. Yang, D.C. Lee, and Y. Kim, "Experimental study on evaporation heat transfer characteristics of R32 in a plate heat exchanger", presented at the 6th World Congr. on Momentum, Heat and Mass Transfer, Lisbon, Portugal, Jun. 17-19, 2021. DOI: 10.11159/icmfht21.lx.106.

[46] X. Huang, J. Zhang, and F. Haglind, "Experimental analysis of high temperature flow boiling of zeotropic mixture R134a/R245fa in a plate heat exchanger", *Appl. Therm. Eng.*, vol. 220, article no. 119652, 13 pages, Feb. 2023. DOI: 10.1016/j.applthermaleng.2022.119652.

[47] J. Huang, T.J. Sheer, and M. Bailey-McEwan, "Heat transfer and pressure drop in plate heat exchanger refrigerant evaporators," *Int. J. Refrig*., vol. 35, no. 2, pp. 325-335, Mar. 2012. DOI: 10.1016/j.ijrefrig.2011.11.002.

[48] G.A. Longo, S. Mancin, G. Righetti, and C. Zilio, "Boiling of the new low-GWP refrigerants R1234ze(Z) and R1233zd(E) inside a small commercial brazed plate heat exchanger", *Int. J. Refrig*., vol. 104, pp. 376-385, Aug. 2019. DOI: 10.1016/j.ijrefrig.2019.05.034.

Table 1 Condensation pressure drop data in plate heat exchangers

Study	Fluid, PHE dimensions, and test conditions	No. of data		% Of Data	Experimental uncertainty (ΔP)	MBD and RMSD (Eq. (1))
		Laminar	Turbulent			
Yan et al. [2]	R134a, A_P = 0.054 m^2, P_{sat} = 7 bar, q" = 10-6 kW/m^2, G = 80 kg/m^2s	79	10	8.9%	±20%	-32% and 57.4%
Kuo et al. [3]	R410A, A_P = 0.054 m^2, P_{sat} = 1.44-1.95 MPa, q" = 5-20 kW/m^2, G = 50-150 kg/m^2s	38	51	8.9%	±16.5%	33.6% and 36.7%
Djordjevic et al. [4]	R134a, A_P = 0.424 m^2, T_{sat} = 27.5°C, q" = 11.5-17.1 kW/m^2, G = 50 kg/m^2s	40	0	4.0%	±20%	-129.3% and 137.5%
Shon et al. [5]	R1233zd(E), A_P = 0.031 m^2,	27	0	2.7%	1.5%	41% and 41.7%

	P_{sat} = 2-3 bar, q" = 2 kW/m^2, G = 19.9-23.8 kg/m^{2}s					
Soontarapiromsook et al. [6]	R134a, A_P = 0.032 m^2, T_{sat} = 40°C and 50°C, q" = 5-15 kW/m^2, G = 61 kg/m^{2}s and 89 kg/m^{2}s	16	1	1.69%	±8.41%	61.7% and 67.3%
Zhang et al. [7]	R134a, R1234ze(E). and R245fa, A_P = 0.024 m^2, T_{sat} = 30-70°C, q" = 0 kW/m^2, G = 53 kg/m^{2}s	119	0	11.85 %	15.2%	34.8% and 41.5%
Kwon et al. [8]	R1233zd(E), A_P = 0.0274 m^2, P_{sat} = 2-3 bar, q" = 2.5-4,5 kW/m^2, G = 19.9 kg/m^{2}s	59	0	5.88%	15.96%	34.6% and 36.3%

	and 23.8 kg/m^{2}s					
Park and Kim [9]	R134a, A_P = 0.06 m^2, T_{sat} = 30-40°C, q" = 6 kW/m^2 and 8 kW/m^2, G = 40-80 kg/m^{2}s	87	2	8.86%	Not available	-14% and 19.9%
Park et al. [10]	R410A, A_P = 0.06 m^2, T_{sat} = 30-40°C, q" = 4-8 kW/m^2, G = 40-80 kg/m^{2}s	53	30	8.27%	Not available	16.8% and 23%
Tao et al. [11]	NH_3, A_P = 0.064 m^2, T_{sat} = 13.4-22.6°C, q" = 0 kW/m^2, G = 21-71 kg/m^{2}s	69	0	6.87%	±15%	-35.1% and 54.9%
Tao and Ferreira [12]	NH_3, A_P = 0.064 m^2, T_{sat} = 13.4-22.6°C, q" = 0 kW/m^2, G = 21-71 kg/m^{2}s	31	0	3.1%	±15%	-34.8% and 54%

Ko et al. [13]	R124, A_P = 0.039 m^2, T_{sat} = 33.74°C and 44.73°C, q" = 2.5-4.5 kW/m^2, G = 16-26 kg/m^2s	27	0	2.69%	3.57%	42.5% and 42.8%
Jung et al. [14]	R124, A_P = 0.0274 m^2, P_{sat} = 7.2 bar and 8.2 bar, q" = 2.5 kW/m^2, G = 26.5 kg/m^2s	10	0	1%	3.14%	40% and 40.7%
Lee et al. [15]	R1234ze(E), A_P = 0.028 m^2, T_{sat} = 15°C, q" = 0 kW/m^2, G = 50-130 kg/m^2s	39	0	3.88%	±7.97%	20.6% and 37.3%
Wang et al. [16]	R365mfc, A_P = 0.167 m^2, T_{sat} = 43°C, q" = 0 kW/m^2, G = 25.35-44.74 kg/m^2s	11	0	1.1%	±17.8%	-39.2% and 58.2%

Hu and Ma [17]	Steam and water/ethanol mixture, A_P = 0.02 m^2, P_{sat} = 0.9 bar, q" = 0 kW/m^2, G = 5.9 kg/m^2s and 14.9 kg/m^2s	205	0	20.4%	±6.64%	-34.7% and 54.7%

Table 2 Predictive correlations for condensation in plate heat exchangers

Study	Deviation		
Equation (1)	MBD	RMSD	Fit
$f_{TP} = 0.112 Re_{LO}^{-0.34} X^{0.1} Co^{0.66} Bd^{0.92} We^{-0.72}$ (x = 0-0.97, G = 5.9-150 kg/m^{2}s, T_{sat} = 13.37-130°C, q" = 0-20 kW/m^2, Re_{LO} = 7-7105, X = (5.58-31,401) x 10^{-4}, Co = (1.6-2868.1) x 10^{-3}, Bd = 0.04-91.15, We = (4.35-21,700) x 10^{-5})	-5.2%	52.1%	R^2 = 0.65 15.7% in ±10%, 44.6% in ±30%, 74.6% in ±50%
Shon et al. [5] $f_{TP} = 1261.1 Re_{eq}^{-0.41} Re_L^{-0.57}$ $G_{eq} = G\left[(1-x) + x\left(\frac{\rho_L}{\rho_V}\right)^{0.5}\right]$ $Re_{eq} = \frac{G_{eq} d_h}{\mu_L}$ $Re_L = \frac{G d_h}{\mu_L}$ (x = 0.2-0.9, G = 13-23.8 kg/m^{2}s, T_{sat} = 37.7-50.9°C, q" = 2.5-4.5 kW/m^2, Re_{eq} = 500-2500, Re_L = 165-198)	-48.5%	164.6%	R^2 = 0.25 7.5% in ±10%, 15.7% in ±30%, and 27.5% in ±50%
Zhang et al. [7] $f_{TP} = 0.0146 Re_{eq}^{0.98} We_{homo}^{-1}$ $We_{homo} = \frac{G^2 d_h}{\rho_m \sigma}$	19.4%	514%	R^2 = 0 2.1% in ±10%, 8.8% in ±30%, and 17.6% in ±50%

$\rho_m = \left(\frac{x}{\rho_V} + \frac{1-x}{\rho_L}\right)^{-1}$ $G_{eq} = G\left[(1-x) + x\left(\frac{\rho_L}{\rho_V}\right)^{0.5}\right]$ $Re_{eq} = \frac{G_{eq} d_h}{\mu_L}$ (x = 0.3-1.0 , G = 16-90 kg/m^{2}s, T_{sat} = 29.7-71.0°C, q" = 4-57.4 kg/m^{2}s, Re_{eq} = 1207-4827)			
Ko et al. [13] $f_{TP} = 1.073 \times 10^6 Re_{eq}^{-1.1} Re_L^{-0.32} Ge^{0.14} \left(\frac{\rho_L}{\rho_V}\right)^{-0.69}$ $G_{eq} = G\left[(1-x) + x\left(\frac{\rho_L}{\rho_V}\right)^{0.5}\right]$ $Re_{eq} = \frac{G_{eq} d_h}{\mu_L}$ $Re_L = \frac{G d_h}{\mu_L}$ $Ge = \left(\frac{\beta}{180}\right)\pi$ (x = 0.3-0.9, G = 16.6-26.6 kg/m^{2}s, P_{sat} = 557.2-790.5 kPa, q" = 2.5-4.5 kW/m^2, Re_{eq} = 649-2171, Re_L = 238-445, Ge = 0.524-1.047)	-398.6%	1157.7%	R^2 = 0.11 14.1% in ±10%, 26.5% in ±30%, and 38.7% in ±50%
Amalfi et al. [18]			

f_{TP} $= 15.698\left(2.125\left(\frac{\beta}{\beta_{max}}\right)^{9.993} + 0.955\right) We_{homo}^{-0.475} Bd^{0.255} \left(\frac{\rho_L}{\rho_V}\right)^{-0.571}$ $We_{homo} = \frac{G^2 d_h}{\rho_m \sigma}$ $\rho_m = \left(\frac{x}{\rho_V} + \frac{1-x}{\rho_L}\right)^{-1}$ $\beta_{max} = 70°$ (x = 0.1-0.8, G = 8.5-100 kg/m^{2}s, T_{sat} = -2°C to 31°C, q" = 0.14-41.1 kW/m^2, Re_L = 33.1-4740, We_{homo} = 0.0267-150, Bd = 2.4-49.1)	-54.2%	165.7%	R^2 = 0.11 7.47% in ±10%, 20.5% in ±30%, and 33.4% in ±50%
Tao and Ferreira [19] $f_{TP} = (4.207 - 2.673\beta^{-0.46})(4200 - 5.41Bd^{1.2}) Re_{eq}^{-0.95} P_r^{0.3}$ (x = 0.1-0.9, G = 2-150 kg/m^{2}s, P_{sat} = 1-24.2 bar, q" = 2.5-66.5 kW/m^2, Re_{eq} = 710-30,000, P_r = 0.004-0.64)	-282.1%	796%	R^2 = 0.58 11.3% in ±10%, 23.9% in ±30%, and 32.6% in ±50%.

Table 3 Condensation heat transfer data for evaluation

Study	Fluid, PHE dimensions, and test conditions	No. of data		% Of Data	Experimental uncertainty	MBD and RMSD (Eq. (1))
		Laminar	Turbulent			
Han et al. [20]	R410A, A_P = 0.055 m^2, T_{sat} = 20°C and 30°C, q" = 4.7-5.3 kW/m^2, G = 34 kg/m^2s	14	0	16.9%	±250 Pa (±1.96% to ±6.67%)	48% and 48.3%
Muller and Kabelac [21]	Water and R134a, A_P = 0.496 m^2, T_{sat} = 25.9°C and 112.3°C, q" = 75.5 kW/m^2, G = 11-56 kg/m^2s	21	0	25.3%	Not available	-2.9% and 25%
Kwon et al. [22]	R1233zd(E), A_P = 0.0274 m^2, P_{sat} = 2-3 bar, G = 13.7 kg/m^2s and 20 kg/m^2s	48	0	57.8%	2.97%	-8.1% and 14.6%

Table 4 Evaporation heat transfer data in plate heat exchangers

Study	Fluid	No. of data		% Of Data	Experimental uncertainty	MBD and RMSD (Eq. (2))
		Laminar	Turbulent			
Yan et al. [23]	R134a, A_P = 0.054 m^2, P_{sat} = 6.75 bar and 8 bar, q" = 11 kW/m^2 and 15 kW/m^2, G = 55 kg/m^2s and 70 kg/m^2s	38	4	2.01%	±3.2%	-38.2% and 79.9%
Kim and Lee [24]	R22 and R410A, A_P = 0.055 m^2, T_{sat} = 5-15°C, q" = 5.5 kW/m^2, G = 27 kg/m^2s	68	0	3.26%	±2.5%	-69.9% and 103.8%
Han et al. [25]	R410A, A_P = 0.055 m^2, T_{sat} = 5-15°C, q" = 5.5 kW/m^2, G = 27 kg/m^2s	52	0	2.49%	±2.5%	23.7% and 28.5%

Hsieh and Lin [26]	R410A, A_P = 0.054 m^2, P_{sat} = 10.8 bar and 12.5 bar, q" = 4 kW/m^2 and 6 kW/m^2, G = 40-80 kg/m^2s	93	67	7.66%	±16.5%	7.94% and 28.4%
Park and Kim [27]	R134a, A_P = 0.073 m^2, T_{sat} = 0-10°C, q" = 4 kW/m^2 and 6 kW/m^2, G = 40-80 kg/m^2s	91	0	4.36%	Not available	-51.1% and 64.9%
Taboas et al. [28]	Ammonia (52%) and water (48%) mixture, A_P = 0.052 m^2, P_{sat} = 7 bar and 15 bar, q" = 30 kW/m^2 and 35 kW/m^2, G = 70-140 kg/m^2s	8	47	2.63%	±18.2%	60.4% and 61%

Khan et al. [29]	Ammonia, A_P = 0.095 m^2, T_{sat} = -2°C to 25°C, q" = 32.5 kW/m^2, G = 5.5 kg/m^2s	35	0	1.68%	±3.0%	-87% and 103.9%
Khan et al. [30]	Ammonia, A_P = 0.095 m^2, T_{sat} = -2°C to 25°C, q" = 6.9-49.1 kW/m^2, G = 8 kg/m^2s and 27 kg/m^2s	53	0	2.54%	±2.6%	-37.3% and 48.7%
Vakili-Farahani et al. [31]	R245fa, A_P = 0.015 m^2, T_{sat} = 25-35°C, q" = 0 kW/m^2, G = 10-40 kg/m^2s	46	0	2.2%	±15%	21.5% and 30.3%
Lee et al. [32]	Water, A_P = 0.0419 m^2, T_{sat} = 103.9°C, q" = 15-30 kW/m^2, G = 14.5-24 kg/m^2s	69	0	3.3%	±1.2%	-8.7% and 0.8%

Khan et al. [33]	Ammonia, A_P = 0.095 m^2, T_{sat} = -2°C to -25°C, q" = 21.2-49.1 kW/m^2, G = 6.5 kg/m^2s	37	0	1.77%	±2.8%	-145.8% and 160.3%
Khan et al. [34]	Ammonia, A_P = 0.095 m^2, T_{sat} = -2°C to -25°C, q" = 21.2-49.1 kW/m^2, G = 6.5 kg/m^2s	14	0	0.67%	Not available	-132% and 151.3%
Amalfi et al. [35]	R245fa, A_P = 0.015 m^2, T_{sat} = 25-30.5° C, q" = 0 kW/m^2, G = 15-45 kg/m^2s	52	0	2.49%	±2.4%	22.9% and 29.7%
Desideri et al. [36]	R245fa and R1233zd(E), A_P = 0.023 m^2, T_{sat} = 100-130°C, q" =	72	2	3.54%	±11.6%	11.2% and 54.2%

	13-97 kW/m^2, G = 68-100 kg/m^{2}s					
Zhang et al. [37]	R134a, R1234ze, and R1234yf, A_P = 0.024 m^2, T_{sat} = 60-80°C, q" = 0 kW/m^2, G = 86-137 kg/m^{2}s	257	17	13.11 %	15.6%	-38.2% and 79.9%
Kim et al. [38]	R1234ze(E), A_P = 0.027 m^2, T_{sat} = 5-15°C, q" = 6.5-10.4 kW/m^2, G = 21.3-58.1 kg/m^{2}s	101	0	4.83%	±3.91%	-69.9% and 103.8%
Lee et al. [39]	R1233zd(E) and R245fa, A_P = 0.0274 m^2, T_{sat} = 60-80°C, q" = 6.5-10.4 kW/m^2, G = 32-58 kg/m^{2}s	45	0	4.13%	±6.43%	-51.5% and 131.6%

Lee et al. [40]	R1234ze(E) (15.47%) and R32 (84.53%) mixture, R32 and R134a, A_P = 0.0274 m^2, T_{sat} = 60-80°C, q" = 6.5-10.4 kW/m^2, G = 32-58 kg/m^2s	37	0	1.77%	±6.75%	44.8% and 48.8%
Song et al. [41]	R245fa, A_P = 0.3423 m^2, A_P = 0.3423 m^2, T_{sat} = 60-80°C, q" = 6-9 kW/m^2, G = 15-30 kg/m^2s	54	0	4.96%	±10.65%	31.2% and 68%
Soontarapiromsook et al. [42]	R134a, A_P = 0.032 m^2, T_{sat} = 20°C, q" = 10 kW/m^2, G = 67-96 kg/m^2s	20	5	1.2%	±8.23%	50.3% and 51.9%
Jo et al. [43]	R1234ze(E), A_P = 0.369 m^2, T_{sat} =	35	0	1.68%	±8.23%	-45.9% and 49.8%

	15°C, q" = 4.1 kW/m^2, G = 20-40 kg/m^{2}s					
Zhang and Haglind [44]	R134a, R1234ze(E), R236fa, R1233zd(E), Propane, and Isobutane, A_P = 0.011 m^2, P_{sat} = 0.165-27.63 bar, q" = 0 kW/m^2, G = 52-137 kg/m^{2}s	126	189	15.08 %	18.2%	-4.7% and 36.4%
Yang et al. [45]	R32 and R410A, A_P = 0.0273 m^2, T_{sat} = 5°C, q" = 6.45 kW/m^2, G = 50-90 kg/m^{2}s	29	1	1.44%	Not available	-0.8% and 33.4%
Huang et al. [46]	R134a (21.6%) and R245fa (78.4%) mixture, R134a (42.7%) and	325	0	15.6%	18.6%	-29.6% and 52.5%

	R245fa (78.4%) mixture, and R134a (63.6%) and R245fa (36.4%) mixture, A_P = 0.021 m^2, P_{sat} = 17.9-27.6 bar, q" = 15.2-39.7 kW/m^2, G = 103-137 kg/m^2s					

Table 5 Predictive correlations for evaporation in plate heat exchangers

Study	Deviation		
Equation (2)	MBD	RMSD	Fit
$f_{TP} = 0.306 Re_{LO}^{0.18} Bd^{0.52} X^{-0.09} We^{-0.63} Co^{0.16} Bo^{0.02} P_r^{-0.48} \left(\frac{\rho_L}{\rho_V}\right)^{-1.24} \left(\frac{\mu_L}{\mu_V}\right)$ (Re_{LO} = 7-4870, T_{sat} = -50°C to 141.5°C, G = 5.5-140 kg/m^{2}s, q" = 0-75.5 kW/m^2, x = 0-1.0, Bd = 0.54-304, X = (5.77-28,830) x 10^{-4}, We = (6.156-111,875) x 10^{-3}, Co = (2.687-3781) x 10^{-3}, Bo = (1-561,400) x 10^{-8}, P_r = 0.00528-0.65)	-15.3%	64.5%	R^2 = 0.71 14.3% in ±10%, 42.7% in ±30%, and 64.9% in ±50%
Khan et al. [30] $f_{TP} = 212 Re_{eq}^{-0.51} P_r^{0.53}$ (Re_{eq} = 1387-2200, T_{sat} = -2°C to -25°C, G = 8.5-27 kg/m^2, q" = 21-44 kW/m^2, x = 0.3-0.95)	-5813%	8129%	R^2 = 0.27 0.1% in ±50%
Song et al. [41] $f_{TP} = 0.0772 Re_{eq}^{0.659}$ (Re_{eq} = 550-3000, T_{sat} = 60-80°C, G = 15-30 kg/m^{2}s, q" = 6-9 kW/m^2, x = 0.1-0.9)	-8550%	36,440%	R^2 = 0.15 0.8% in ±10%, 2.5% in ±30%, and 2.9% in ±50%
Soontarapiromsook et al. [42]			R^2 = 0.11 9.81% in

$f_{TP} = 5.703 Re_{eq}^{-0.133} \left(\frac{\varepsilon}{d_h}\right)^{0.089}$ ($\varepsilon = 0.594\ \mu m$) ($T_{sat}$ = 10-20°C, G = 67-96 kg/m^{2}s, q" = 5-15 kW/m^2, x = 0.1-0.9)	-176%	1001%	±10%, 26.8% in ±30%, and 39.7% in ±50%
Huang et al. [46] $f_{TP} = 0.0621 Re_{eq}^{0.3281} Re_L^{-0.0628}$ (P_{sat} = 17.9-27.4 bar, G = 103-137 kg/m^{2}s, q" = 15.2-39.7 kW/m^2, x = 0.33-0.72)	-140%	980.5%	R^2 = 0.19 3.9% in ±10%, 17.8% in ±30%, and 37.5% in ±50%
Huang et al. [47] $f_{TP} = \frac{3.81 \times 10^4 \times F_{RF}}{\left(Re_{TP}^{0.9} \times \left(\frac{\rho_L}{\rho_V}\right)^{0.16}\right)}$ $R = \frac{\beta}{30°}$ $F_{RF} = 0.183R^2 - 0.275R + 1.10$ (T_{sat} = 5.9-13°C, G = 10.7-31.4 kg/m^{2}s, q" = 0 kW/m^2, x_{out} = 0.24-0.95, β = 28-60°)	-1268%	2289%	R^2 = 0.17 0.5% in ±10%, 1.7% in ±30%, and 3.6% in ±50%

Table 6 Evaporation heat transfer data for evaluation

Study	Fluid	No. of data		% Of Data	Experimental uncertainty	MBD and RMSD (Eq. (2))
		Laminar	Turbulent			
Amalfi et al. [35]	R245fa, A_P = 0.015 m^2, T_{sat} = 25-30.5° C, q" = 0 kW/m^2, G = 15-45 kg/m^2s	47	0	53.4%	±2.4%	22.9% and 29.7%
Longo et al. [48]	R1234ze(Z) and R1233zd(E), A_P = 0.02 m^2, T_{sat} = 30-40°C, q" = 12.15 kW/m^2, G = 5.6-25.6 kg/m^2s	41	0	46.6%	Not available	9.9% and 39.1%

List of Figure Captions

Figure 20 Validation of Eq. (2) with widely reported [35] and independent [48] data

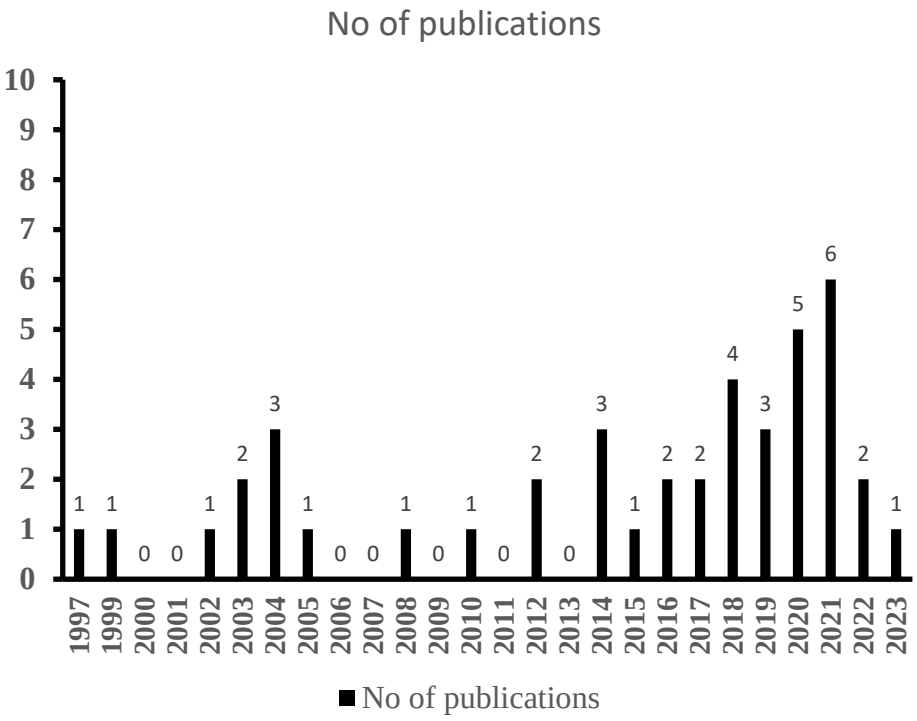

Figure 1 Publication record by year

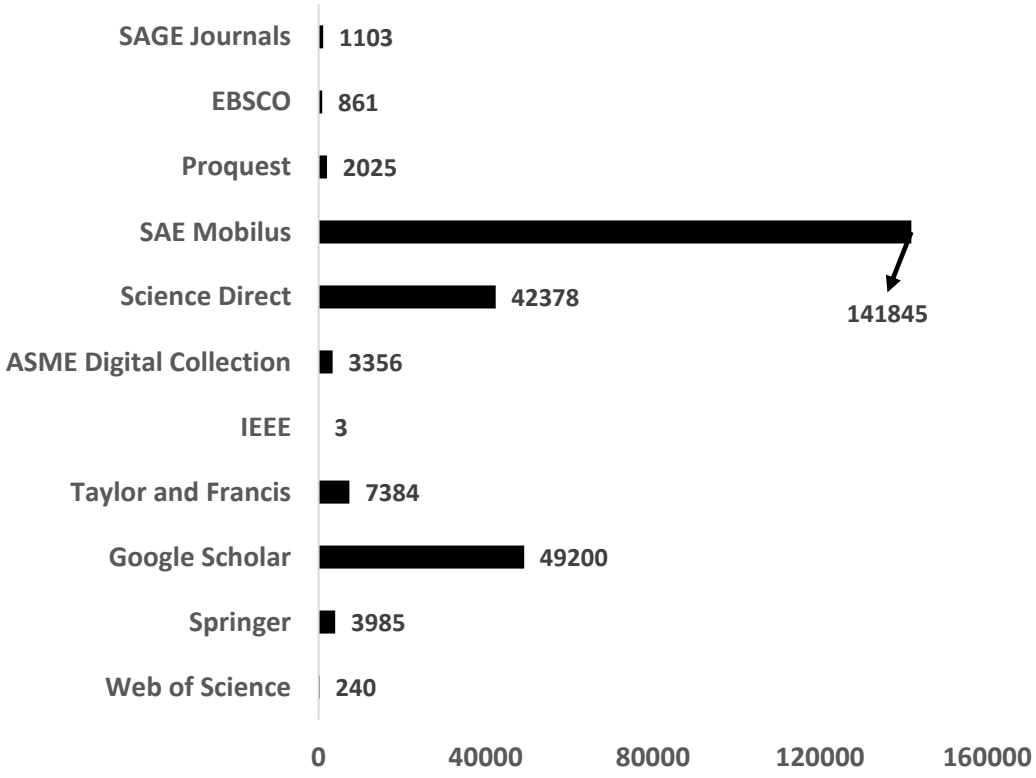

Figure 2 Database search by source and number of records

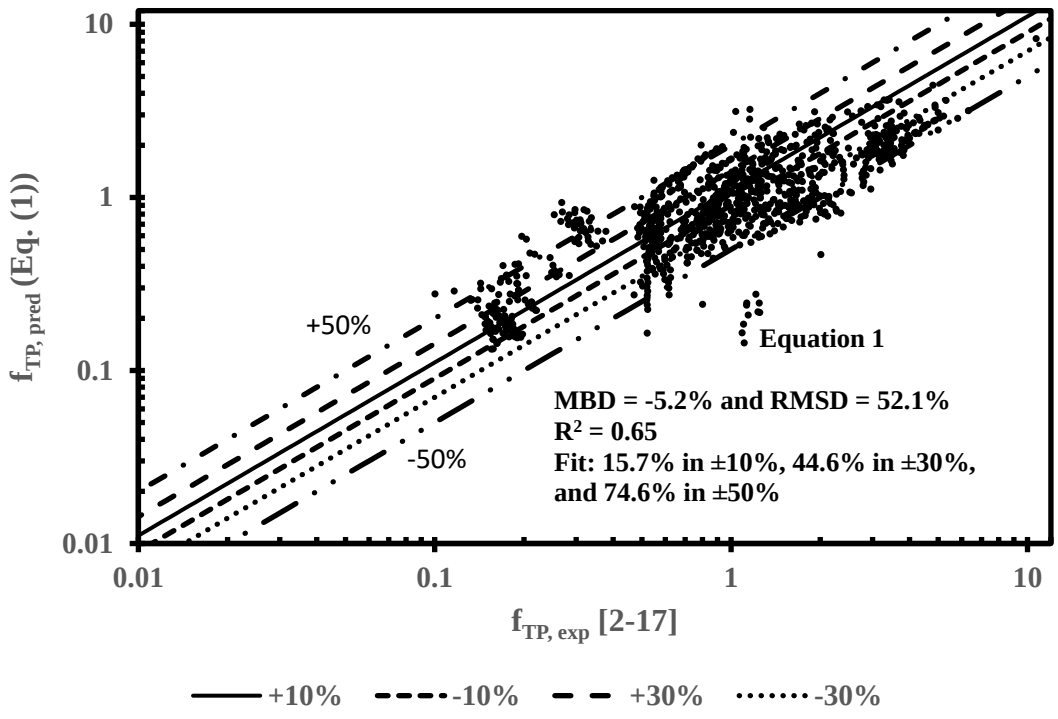

Figure 3 Predictive correlation for the two-phase friction factor in PHE condensers

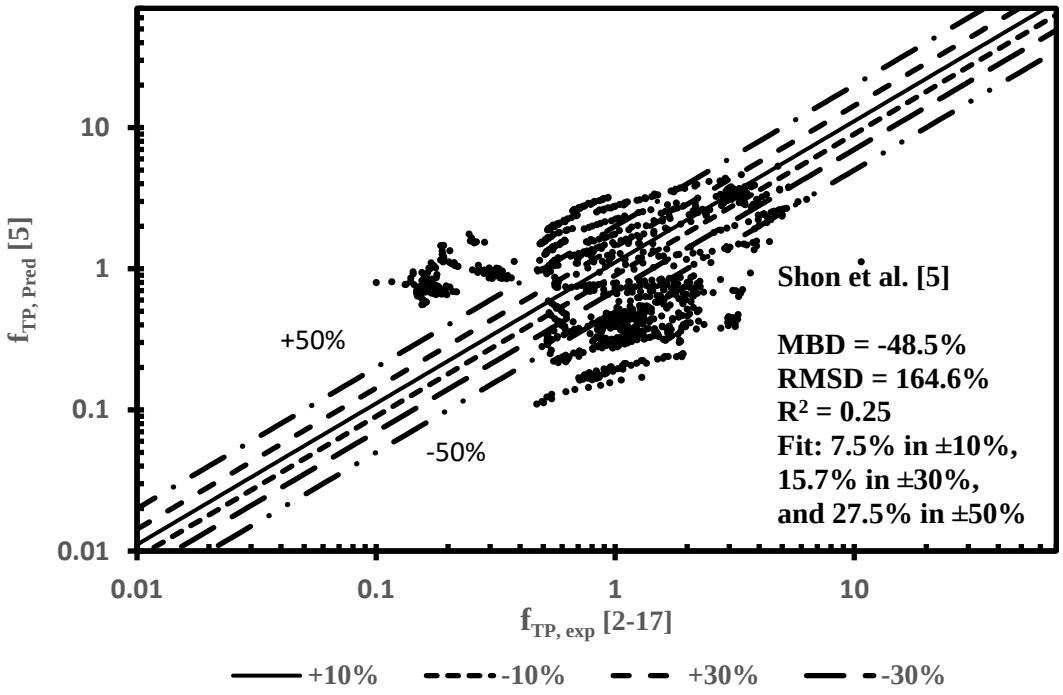

Figure 4 Comparison with the Shon et al. [5] correlation

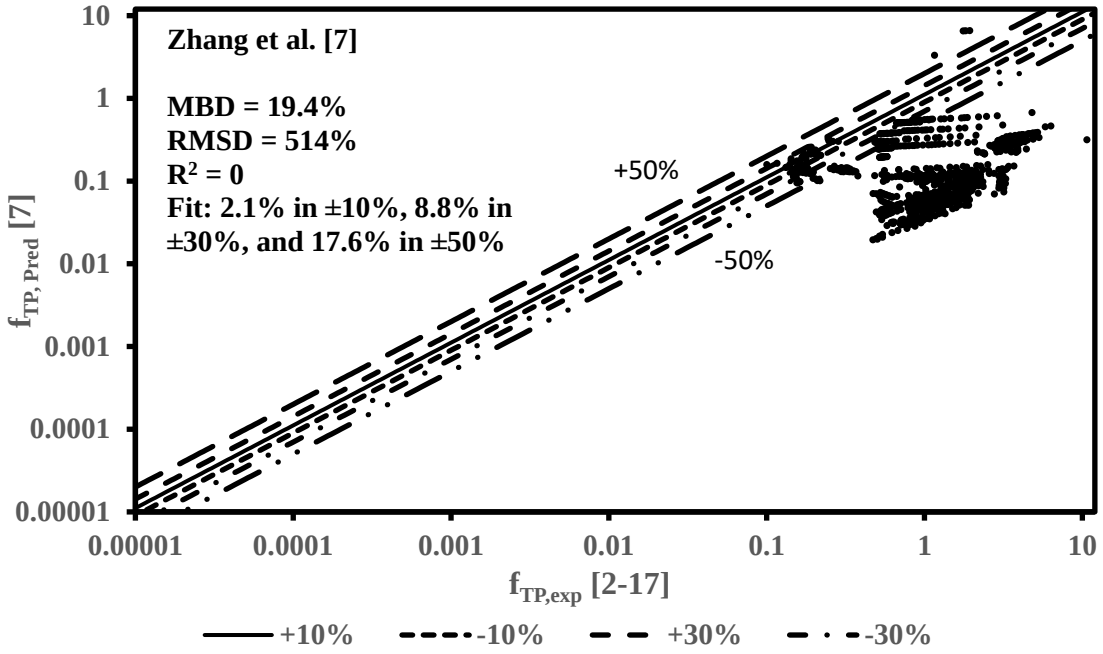

Figure 5 Comparison with the Zhang et al. [7] correlation

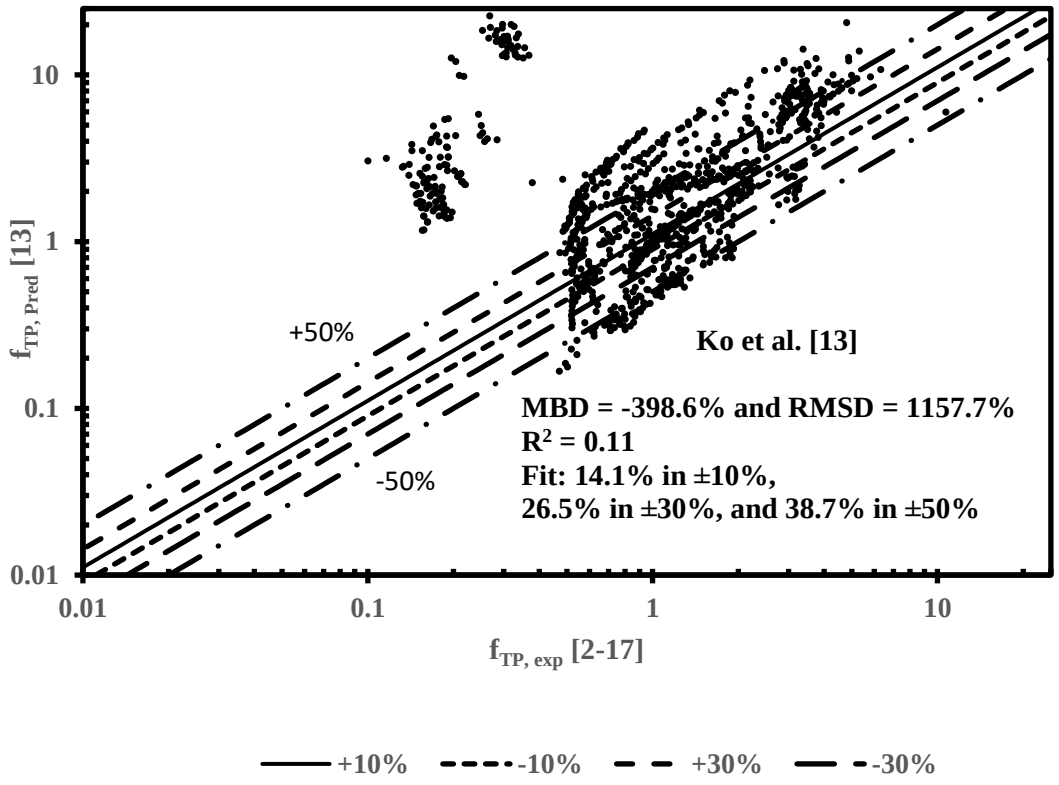

Figure 6 Comparison with the Ko et al. [13] correlation

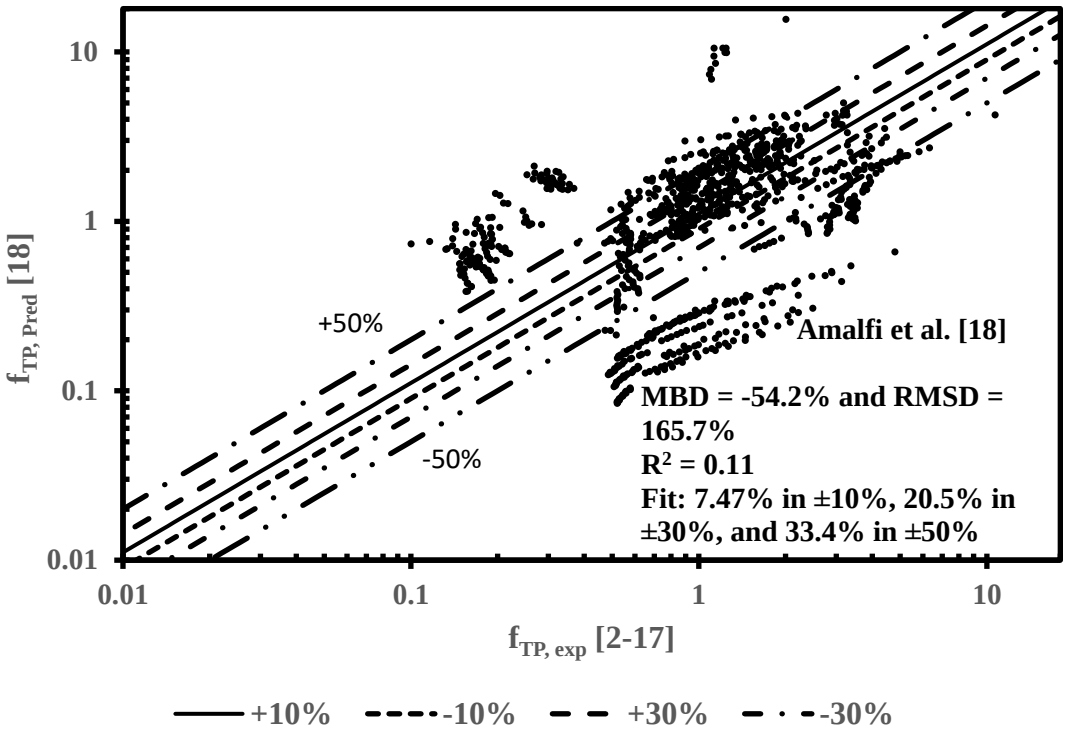

Figure 7 Comparison with the Amalfi et al. [18] correlation

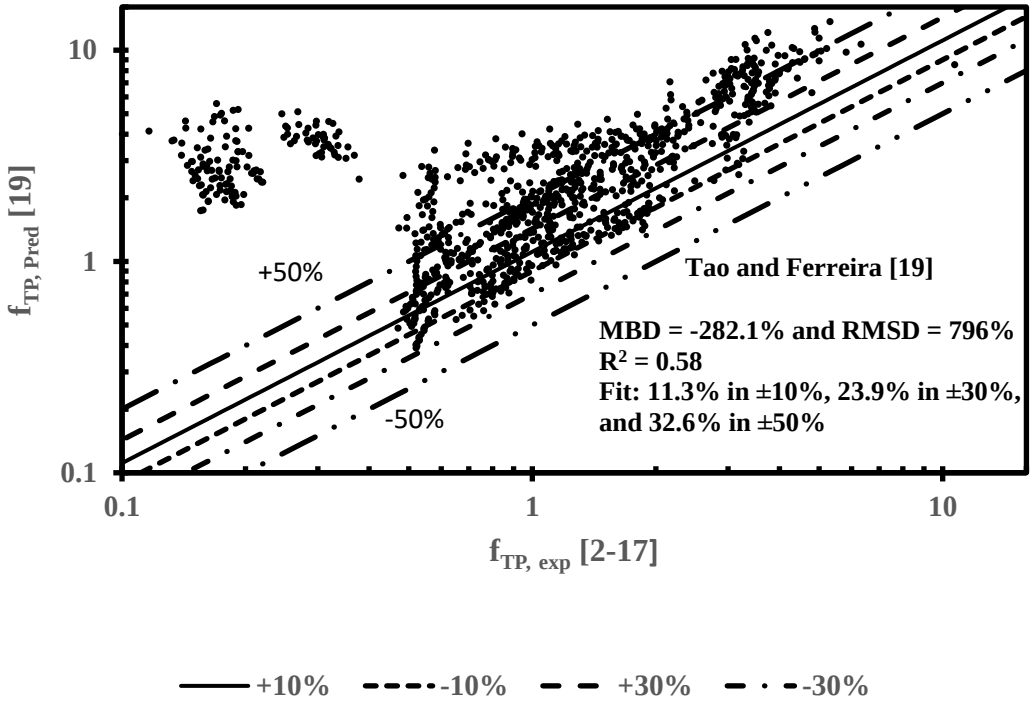

Figure 8 Comparison with the Tao and Ferreira [19] correlation

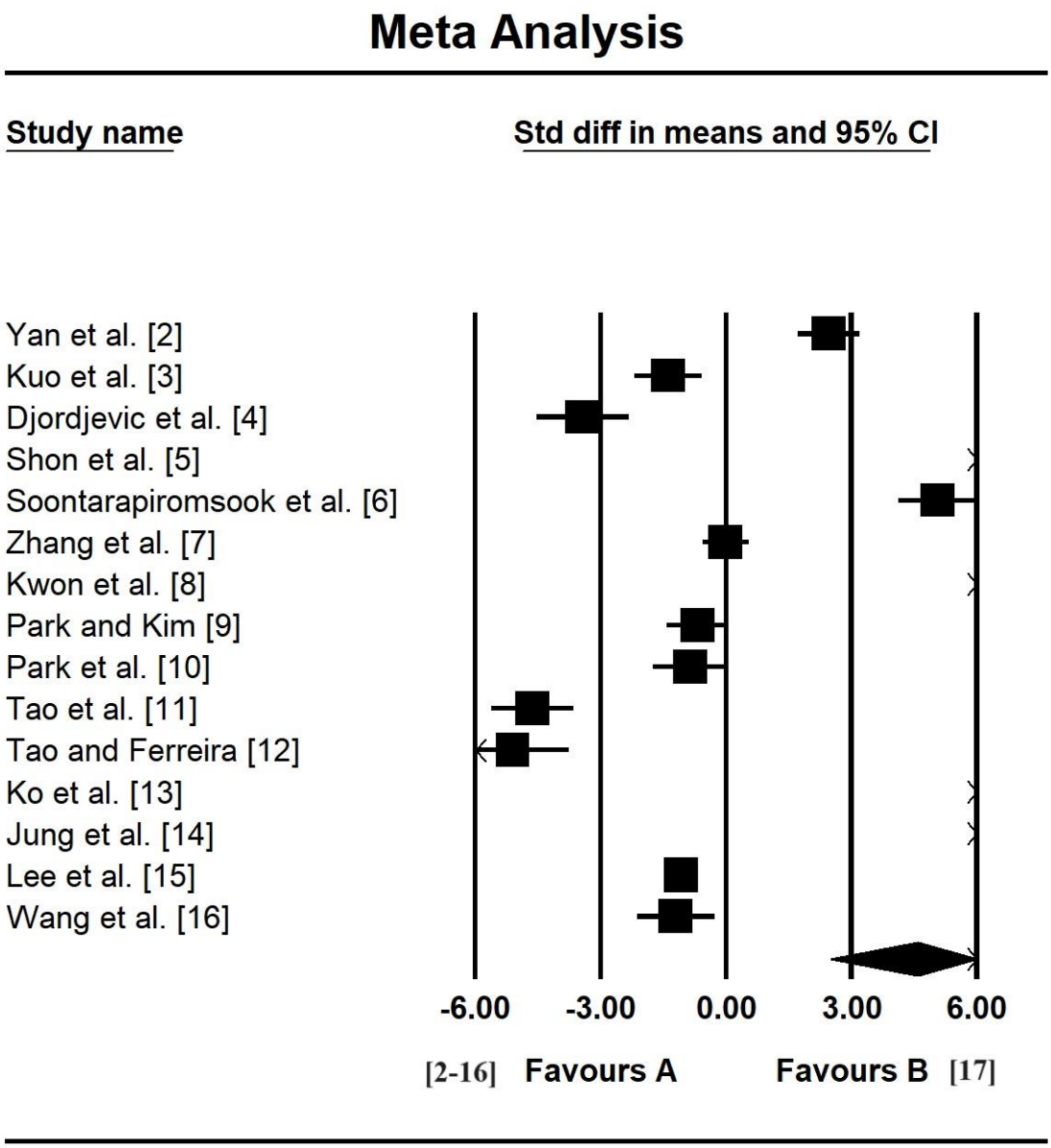

Figure 9 Meta-analysis of the condensation pressure drop data [2-17]

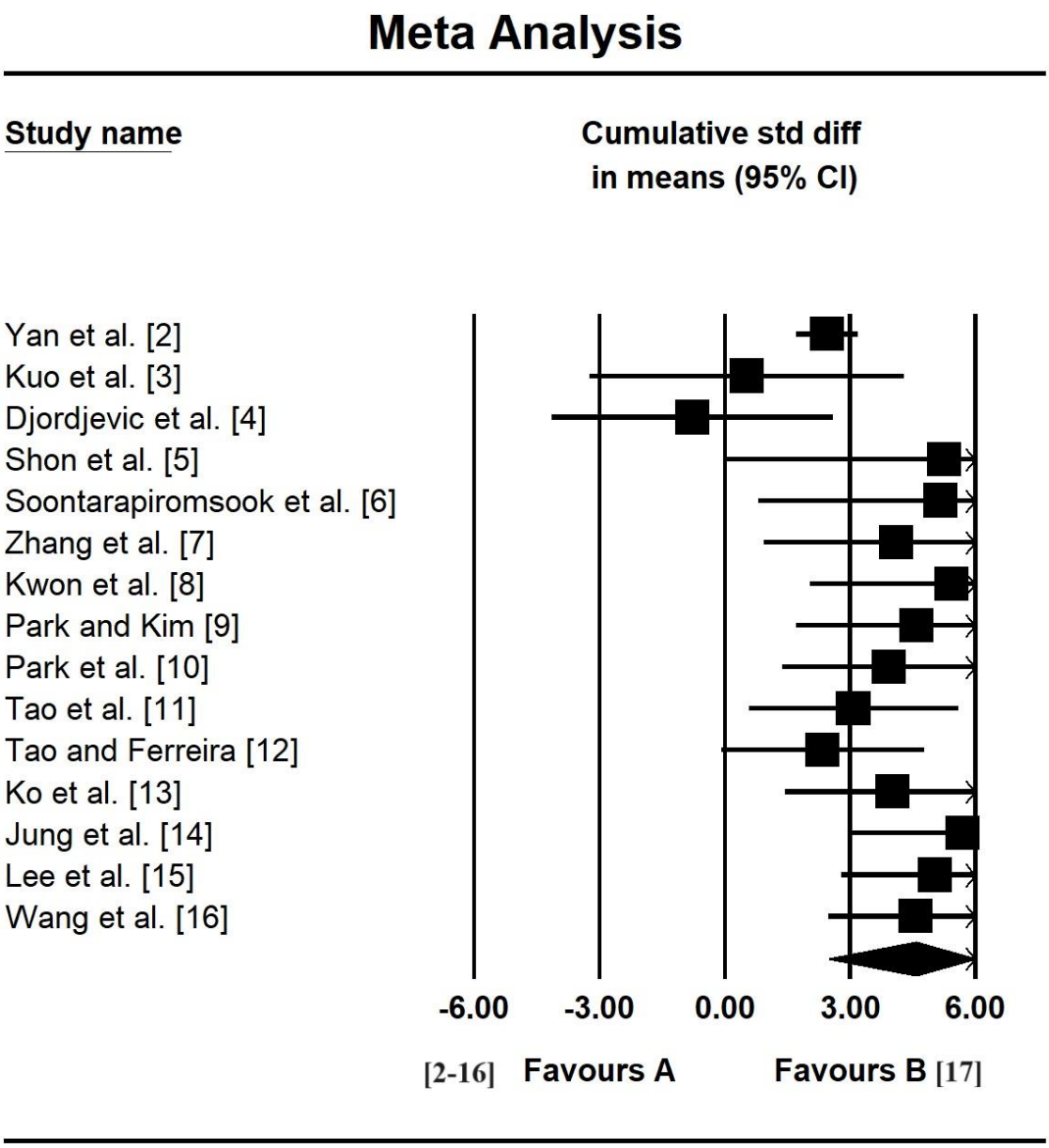

Figure 10 Cumulative Meta-analysis of the condensation pressure drop data [2-17]

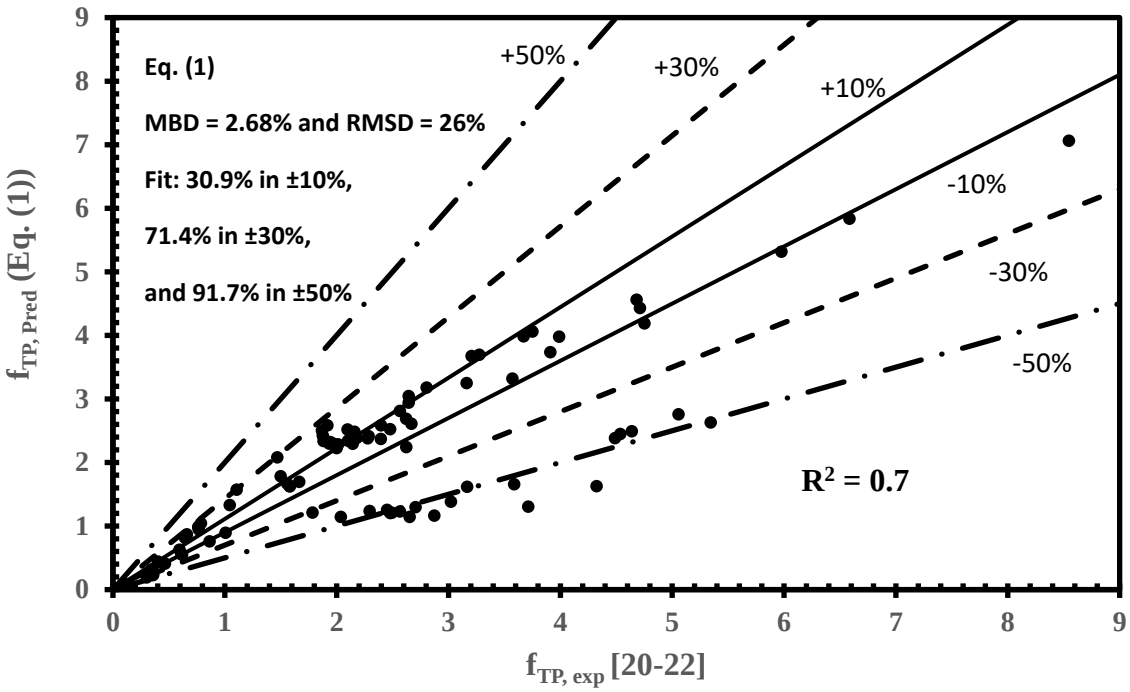

Figure 11 Evaluation of Eq. (1) with independent data [20-22]

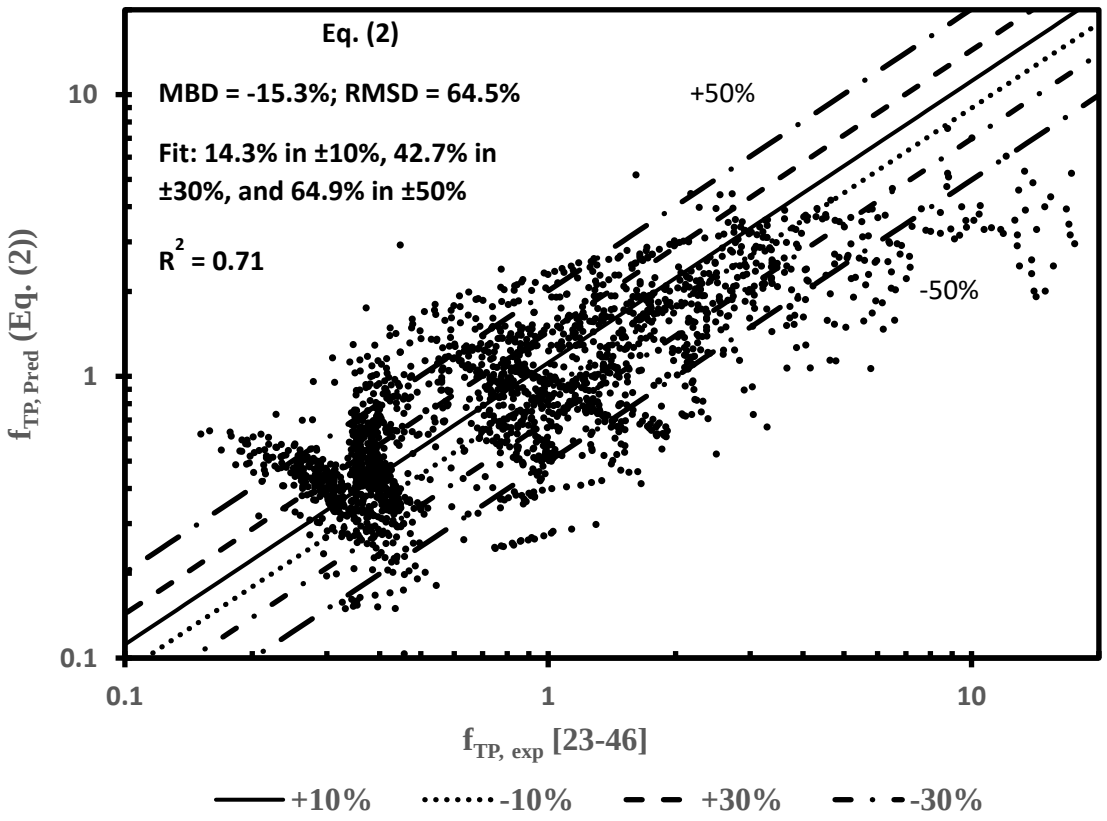

Figure 12 Predictive correlation for the two-phase friction factor in PHE evaporators

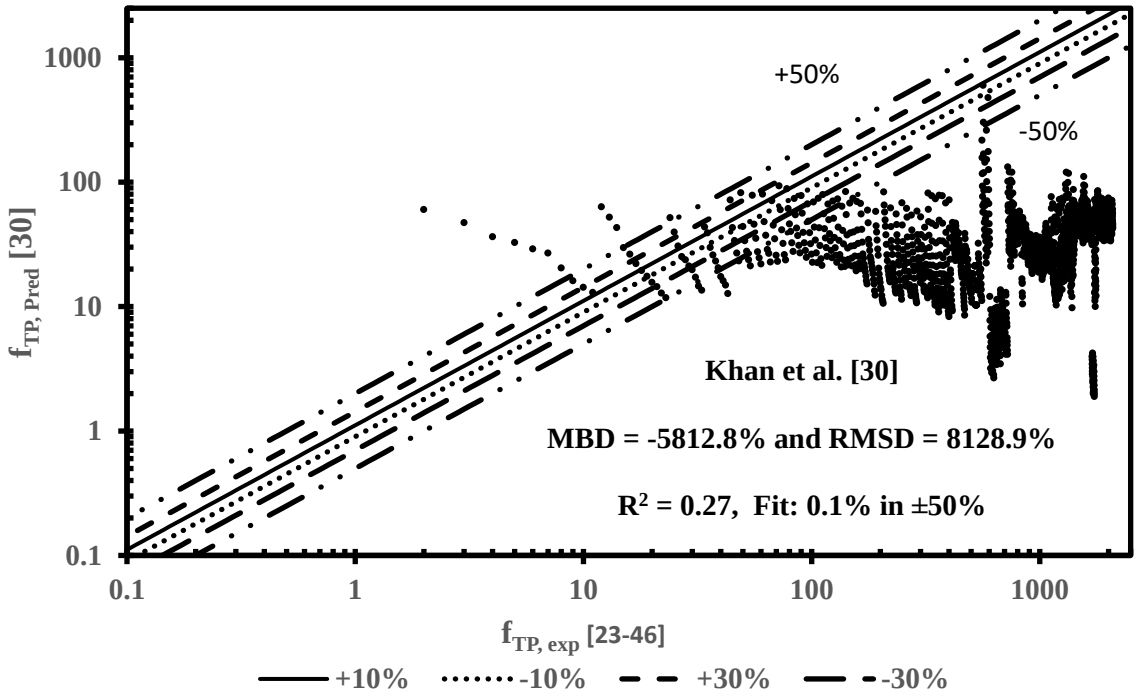

Figure 13 Comparison with the Khan et al. [30] correlation

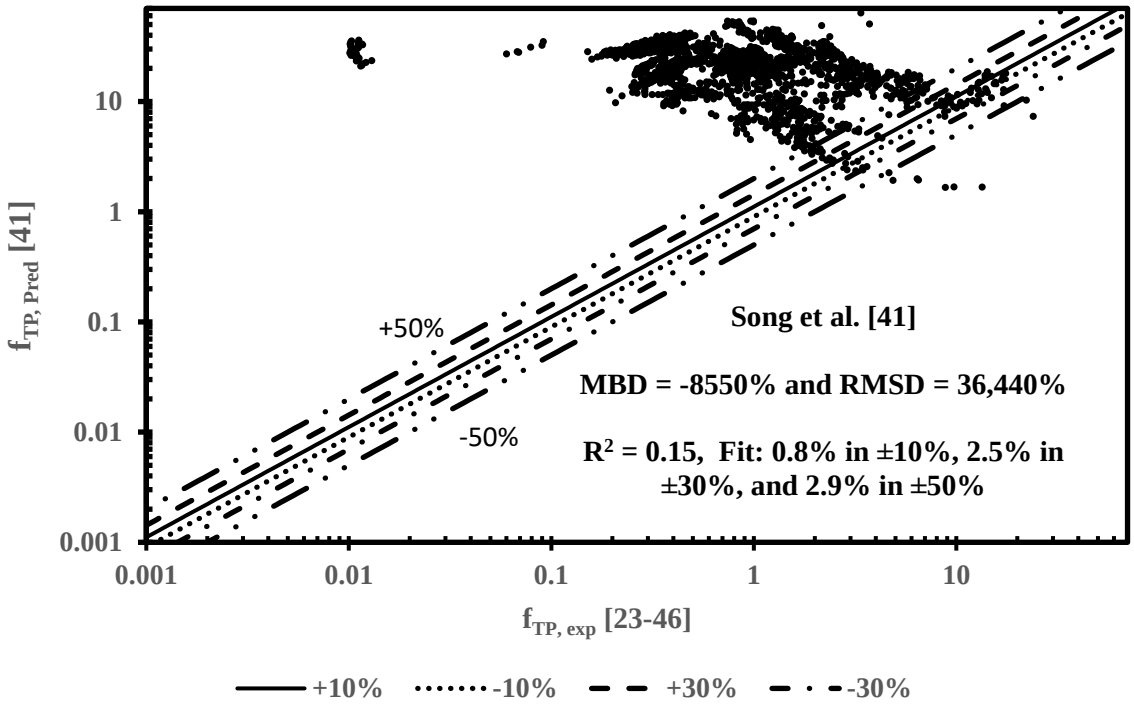

Figure 14 Comparison with the Song et al. [41] correlation

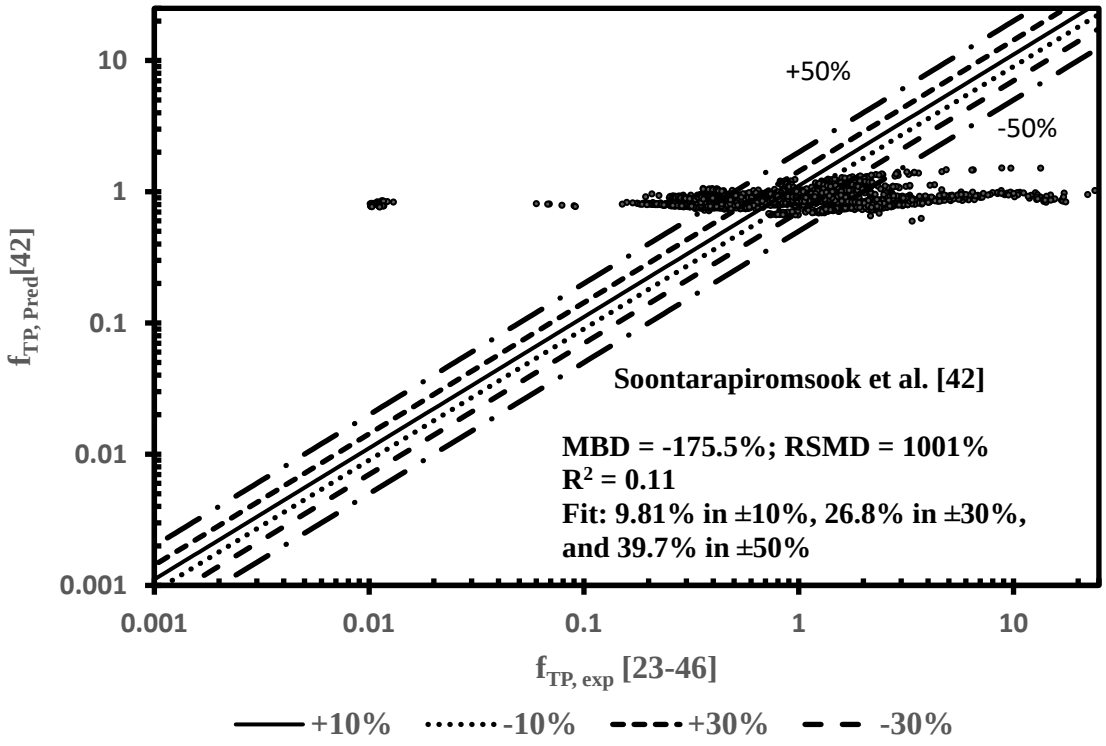

Figure 15 Comparison with the Soontarapiromsook et al. [42] correlation

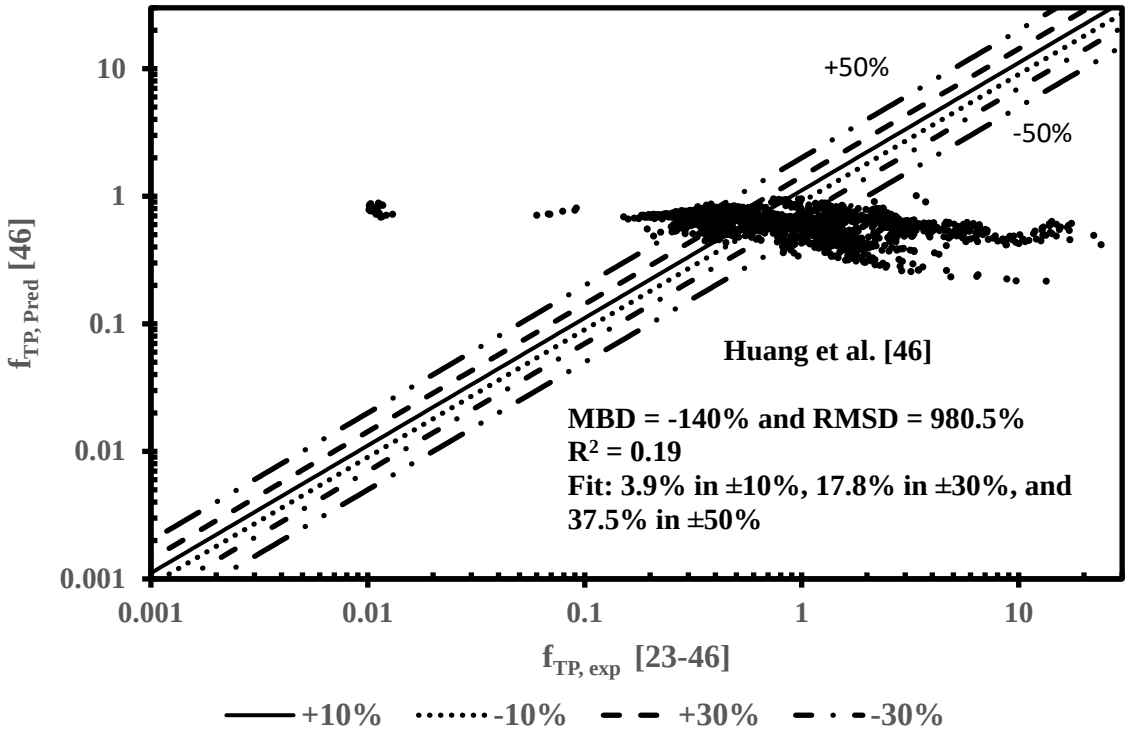

Figure 16 Comparison with the Huang et al. [46] correlation

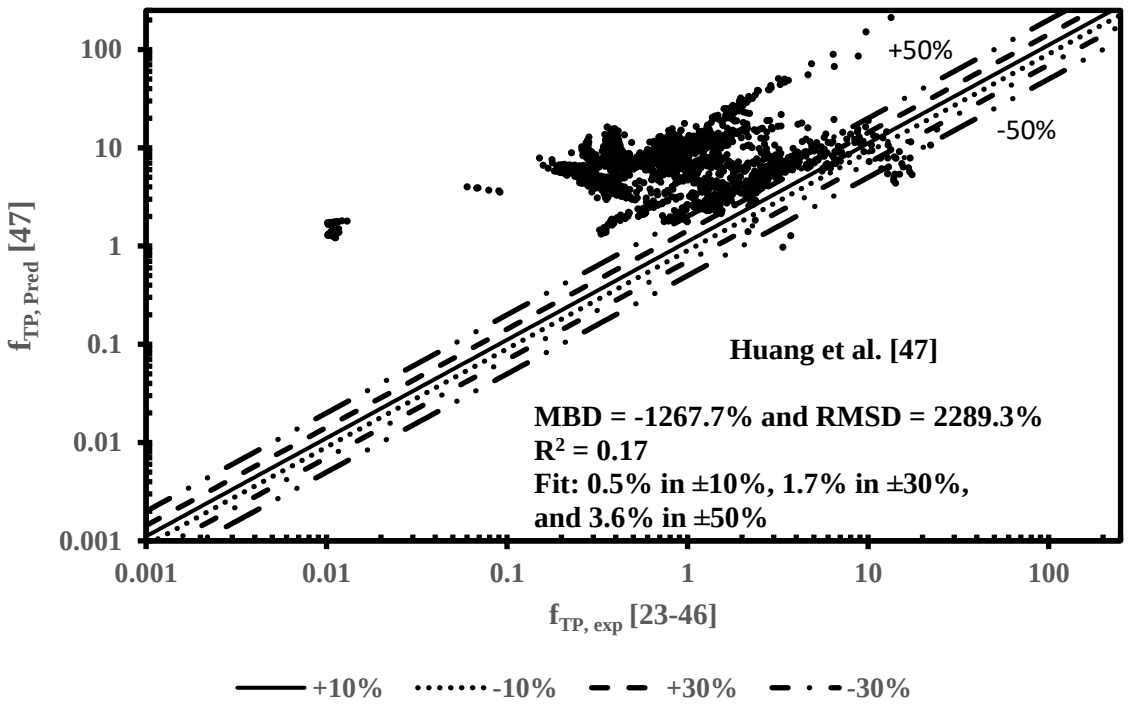

Figure 17 Comparison with the Huang et al. [47] correlation

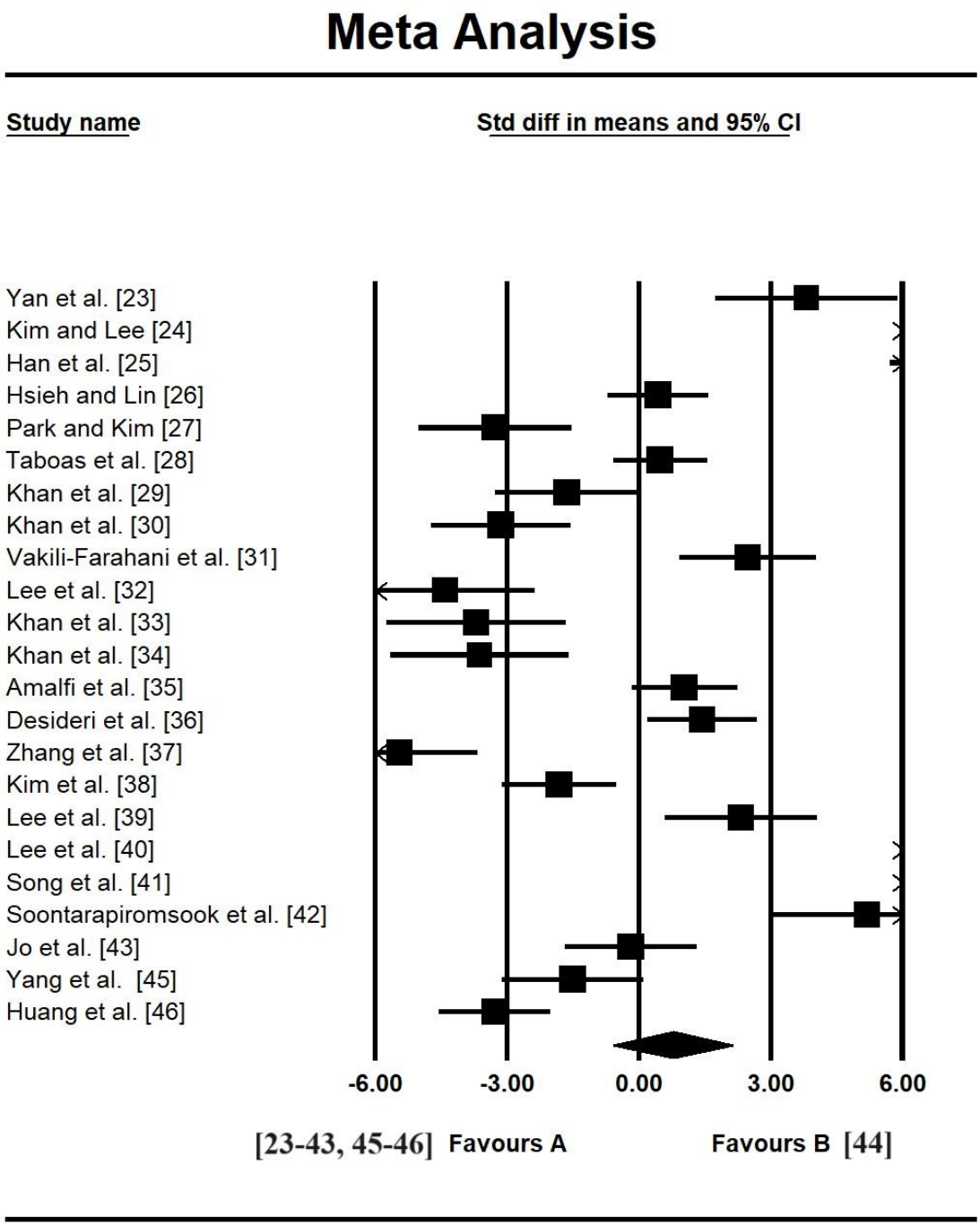

Figure 18 Meta-analysis of the evaporation pressure drop data [23-46]

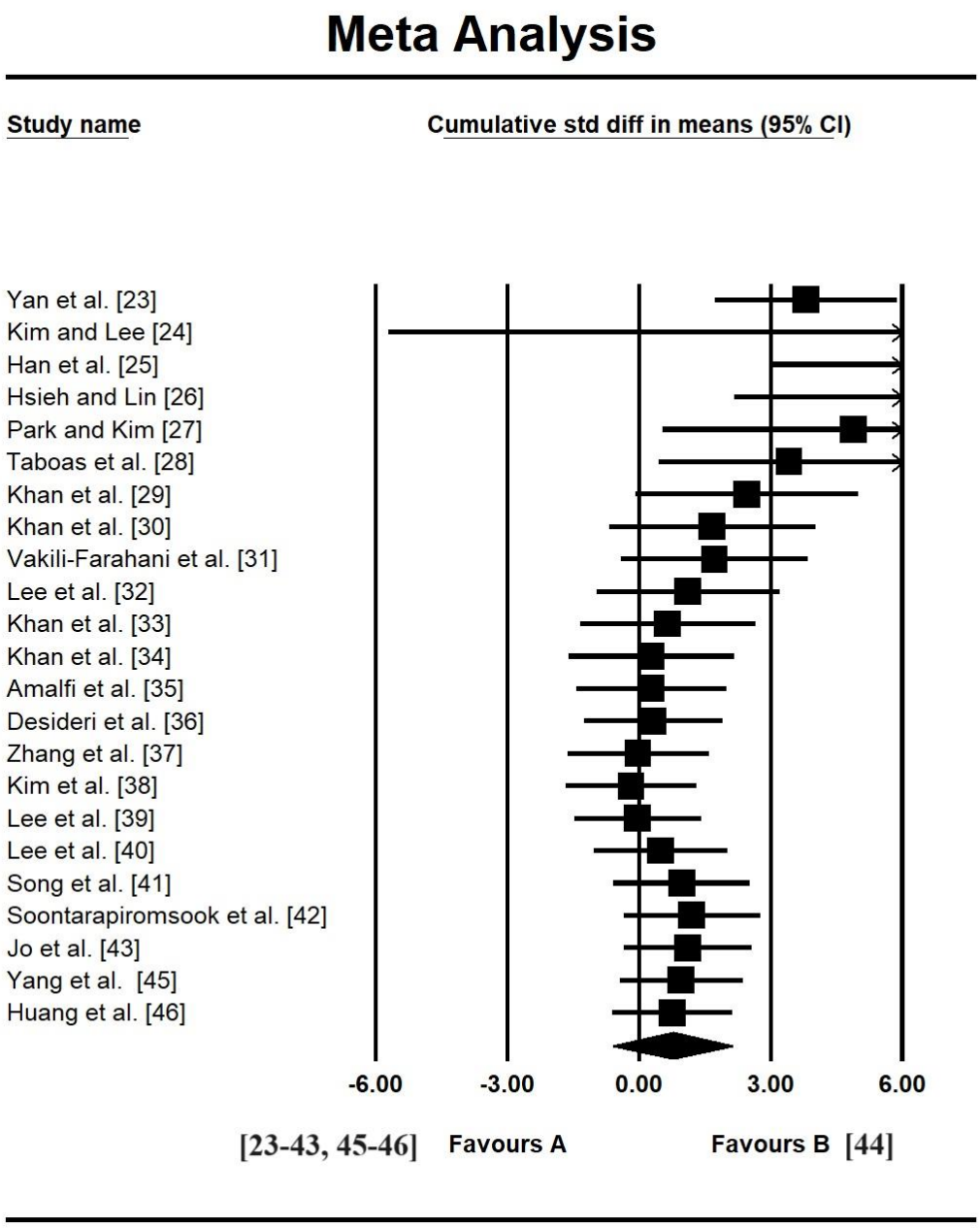

Figure 19 Cumulative meta-analysis of the evaporation pressure drop data [23-46]

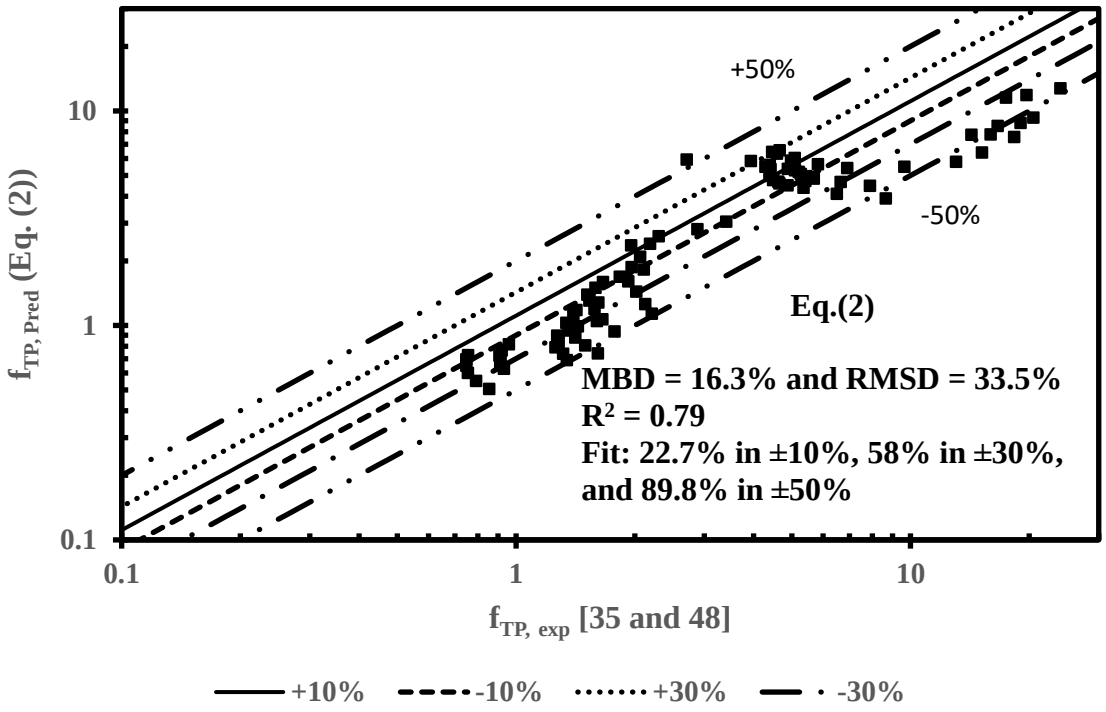

Figure 20 Validation of Eq. (2) with widely reported [35] and independent [48] data

Notes on Contributors

Yagnavalkya Mukkamala. Professor Mukkamala received his Ph.D. in Mechanical Engineering from Vellore Institute of Technology in 2008 and his M.S. in Mechanical Engineering from Virginia Polytechnic Institute and State University in 1993. He has published over seventeen articles in various peer-reviewed journals and peer-reviewed conference articles. He has completed several funded projects as a principal investigator for the Government of India and numerous as a student investigator for the US Department of Energy and NASA. He has been cited over two hundred and ten times and has an h-index of over eight. His research interests include enhanced heat transfer, the design of enhanced heat exchangers, and automotive aerodynamics.

Professor Jaco Dirker is an Associate Professor in Mechanical Engineering at the University of Pretoria. He received his Ph.D. from Rand Afrikaans University (University of Johannesburg) in 2004. He has published over 44 peer-reviewed journals and 44 peer-reviewed conference articles. He has completed over five research projects, with the most recent project being funded by the Royal Society of the United Kingdom for over R 9 million (South African Rand). He is a clean energy and enhanced heat transfer specialist and has supervised several doctoral theses and post-doctoral scholars. He is a registered professional engineer at the Engineering Council of South Africa.